

1 The QCD Running Coupling

Alexandre Deur^a

^aThomas Jefferson National Accelerator Facility, Physics Division, Newport News, VA 23606, USA

© 20xx Elsevier Ltd. All rights reserved.

Contents

1	The QCD Running Coupling	1
	Nomenclature	2
	Objectives	2
1.1	Introduction and Overview	2
1.2	Force couplings, and why they run	3
1.3	Behavior of α_s at high-energy	5
1.4	Methods of determinations of α_s at short distances	9
1.5	Long distance behavior of α_s	11
1.6	Effective charge method	13
1.7	Holographic Light-Front QCD	14
1.8	Dyson-Schwinger equations	15
1.9	Summary and Perspective	15
	Acknowledgments	16
	References	16

Abstract

We describe the coupling of the strong force. Denoted as α_s , it sets the strength of that force, just as G or α specify the strength of the gravity and electromagnetism. Its value depends on the scale at which phenomena are observed. In this chapter, we will explain the nature of the coupling, the quantum origin of its scale dependence, and the crucial consequences this entails for quantum chromodynamics, the gauge theory for the strong force. We describe the theories for the calculation of α_s , using the perturbative method at high-momentum scales (equivalently, short-distance scales) and nonperturbative approaches at low-momentum scales (equivalently, long-distance scales). We also present the experimental determinations of α_s at both short and long distance scales.

Keywords: Strong Force, QCD, running coupling, perturbative, nonperturbative

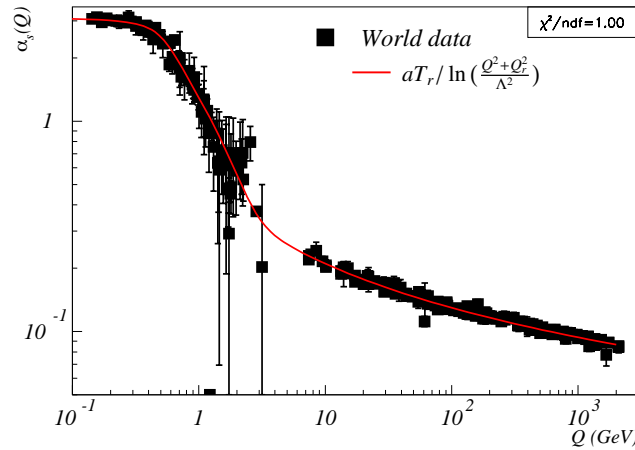


Fig. 1: The QCD coupling, α_s , in function of momentum scale Q . The points are experimental data. The red line is simple fit using the 1-loop perturbative formula $\propto 1/\ln(Q^2/\Lambda^2)$, a Fermi-Dirac function for the scale $Q_r = b/(e^{(Q^2 - c)/d} + 1)$ regularizing the divergence at $Q = \Lambda$, and another Fermi-Dirac function $T_r = (1 + (\pi - 1)e^{(Q - f)/g})$ to smooth the low-to-high Q transition. The parameters values yielding $\chi^2/n.d.f. = 1.00$ are: $a = 1.56$, $\Lambda = 0.246$ GeV, $b = 0.808$ GeV, $c = 0.11$ GeV², $d = 0.20$ GeV², $f = 0.129$ GeV and $g = 0.59$ GeV.

Nomenclature

AdS/CFT	anti-de Sitter/conformal field theory
AdS/QCD	anti-de Sitter/QCD
CEBAF	Continuous Electron Beam Accelerator Facility
CERN	European Organization for Nuclear Research
CLAS	CEBAF Large Acceptance spectrometer
CSR	commensurate scale relations
DESY	Deutsches Elektronen-Synchrotron
DGLAP	Dokshitzer–Gribov–Lipatov–Altarelli–Parisi
DIS	deep inelastic scattering
DSE	Dyson-Schwinger equation
EIC	electron ion collider (at Brookhaven National Laboratory)
EicC	electron ion collider in China
FLAG	flavor lattice averaging group
HERA	Hadron-Electron Ring Accelerator
HLFQCD	holographic light-front QCD
IR	infrared (physics/phenomena)
JLab	Thomas Jefferson National Accelerator Facility
LEP	Large Electron-Positron collider
LF	Light Front
LGT	lattice gauge theory
LHC	large hadron collider (at CERN)
LO	leading order
MOM (scheme)	momentum space subtraction (scheme)
MS (and $\overline{\text{MS}}$)	Minimal Subtraction
NLO (and N^lLO)	next to ... leading order
PDG	Particle Data Group and associated publications
pQCD	perturbative QCD
QCD	quantum chromodynamics
QED	quantum electrodynamics
QFT	quantum field theory
RGE	renormalization group equation
RS	Renormalization Scheme
STI	Slavnov-Taylor Identities
SU(N)	special unitary (group of degree n)
UV	ultraviolet (physics/phenomena)

Objectives

- Origin of the running of the couplings specifying the strength of forces.
- Behavior of the QCD coupling α_s at high-energy, *viz* in the QCD perturbative domain.
- Behavior of α_s at low-energy, *viz* in the QCD nonperturbative domain.
- Methods to determine α_s from experiments or theories.

1.1 Introduction and Overview

The strong force, which binds quarks together into hadrons, and nucleons into nuclei, is one of the four known basic interactions of nature. The three others are electromagnetism, the weak force, and gravity. A crucial attribute of forces is their magnitude, that is, how strongly they act at a given distance and for a given amount of matter. This magnitude is set by the *coupling constant*, *e.g.*, for gravity, Newton's constant G . The strong force coupling constant is named α_s . The quantum field theory (QFT) of the strong force is quantum chromodynamics (QCD). Just like the source of the electromagnetism is the electric charge, the QCD sources are the *color charges*. They come in three types: red, green and blue, in contrast to electromagnetism with its single type of electric charge. Color charges are carried by both quarks and gluons, again unlike in electromagnetism where photons are electrically neutral. Quarks carry one color, anti-quarks one anti-color (anti-red, anti-green or anti-blue), and gluons, one color and one anti-color. Then, according to QCD, the strong force is the effect felt by quarks when they trade colors *via* gluons, with α_s giving the gluon emission probability. Since gluons are also colored, they interact among themselves, with α_s playing the same rôle as in the quark case.

In classical physics, a force coupling *constant* is indeed a fixed number. This is not so in the quantum realm. From symmetry viewpoint, the cause is the appearance of a *quantum anomaly*. From the process viewpoint, the cause is quantum loops, these ephemeral materialization

and subsequent annihilation of pairs of particle-antiparticle. This happens as follows: classically, a fundamental force between two bodies obeys the inverse-square law. However, once matter is scrutinized at short distances where quantum effects become important, quantum loop effects starts to be felt. This causes the force to deviate from the inverse-square law and makes QFT calculations diverge, requiring a *renormalization program*. It is natural in the renormalization process to preserve the inverse-square law and assign to coupling constants the extra distance-dependence from quantum loops, thereby making the hitherto constant couplings scale-dependent. Henceforth, we will thus refer to them simply as *couplings*, while their acquired scale dependence is referred to as their *running*.

For the electric force, the running of the coupling, α , is small: from macroscopic distances to the shortest ones probed in high-energy physics, α increases by about 10% of its value. In contrast, the running is large for α_s , its value changing by several folds. Another crucial difference with α is that while the latter increases as distances decrease, α_s does the opposite: it decreases and even vanishes in the zero-distance limit, see Fig. 1. This phenomenon, known as quark *asymptotic freedom*, is crucial since a small α_s makes the powerful method of perturbation theory available. This availability for QCD at short distances means that the phenomenology of α_s is well understood there. In practice, challenges and uncertainties remain stemming from the facts that (A) high-order perturbative QCD (pQCD) calculations are difficult due to the non-abelian nature of QCD that makes it non-linear; and (B) pQCD provides the running of α_s but not its absolute magnitude. The latter is determined experimentally or using nonperturbative techniques. The consequence of (A) and (B) is that significant theoretical and experimental uncertainties are associated with α_s . For comparison, α is known with a precision of about 1 part in 10 billion, while for α_s at short distance, it is currently about 1%, *viz* 10^8 times worse. This notwithstanding, the nature of α_s and its evolution is well understood in the pQCD domain. Another crucial rôle of α_s is as the expansion parameter for pQCD calculations. Hence, knowing α_s precisely is essential for achieving the accuracy demanded by high-energy scattering experiments, *e.g.*, those at CERN's LHC, which test the Standard Model and explore its expected extension. Currently, a sub-percent precision on α_s is required so that this uncertainty does not dominate other ones. Such precision is presently barely achieved ($\Delta\alpha_s/\alpha_s = 0.85\%$) by combining the world data on α_s [1]. This explains why measuring α_s at short distances remains an active and important sector of research.

At distances similar to hadron sizes, α_s becomes too large to allow for perturbation theory. This has historically clouded our understanding of α_s at long-distance, with predictions on the latter ranging from it vanishing again to being infinite. It was eventually realized that to good approximation, α_s is measurable in that domain. The data were followed by several nonperturbative predictions consistent with the data. All this revealed that at long distances, α_s stops running and is relatively large (Fig. 1). Knowing α_s at long distances allowed for successful predictions of many basic hadronic quantities. The ability to conduct such calculations cannot be overstated since in nature, most phenomena involving QCD are nonperturbative. For example, nonperturbative QCD produces almost all of the universe visible mass.

1.2 Force couplings, and why they run

Classically, the magnitude of a force is characterized by its *coupling constant*, a universal factor that quantifies the force between two static elementary sources. The sources are the elementary electric charge e for electromagnetism, the color charge g for QCD, and the weak isospin g_w for the weak force. For gravity, there is presently no known elementary mass; therefore, its coupling constant G has a $1/\text{mass}^2$ dimension (in natural units, $\hbar = 1 = c$). In contrast, α , α_s , and the weak coupling α_w are dimensionless. Accordingly, and except gravity, a coupling is by definition proportional to the elementary charge squared: $\alpha \equiv e^2/4\pi$, $\alpha_s \equiv g^2/4\pi$ and $\alpha_w \equiv g_w^2/4\pi$. (With the electroweak unification, the weak coupling can be expressed in terms of α and the Weinberg angle θ_w : $\alpha_w = \alpha/\sin^2\theta_w$.)

For linear theories, *i.e.*, those for which the field superposition principle holds, and for static sources emitting a massless field, the coupling is the magnitude-setting factor \mathcal{A} that relates the force to the charges c_1 and c_2 of two sources divided by r^2 , where r is the source separation: $F = \frac{\mathcal{A}c_1c_2}{r^2}$, see Fig. 2. The $1/r^2$ law was first understood by Faraday as the dilution of the force flux as it uniformly expands through 3D space. In QFT, the $1/r^2$ law stems from the propagator of the massless gauge boson carrying the force in the Born approximation *viz*, by one-boson exchange, the leading order (LO) in perturbation theory. In momentum space, this yields the familiar propagator formula $\propto 1/q^2$, where q is the boson 4-momentum.¹ Faraday's picture agrees with the QFT interpretation since a propagator expresses the particle's probability to travel from here to there, and the gauge bosons are emitted isotropically from their source. Yet, when scrutinized in detail, the Born approximation fails: higher orders in perturbation are necessary and alter the $1/r^2$ law. In particular, higher-order diagrams containing loops of particles seemingly yield infinities. Those are managed by regularization and renormalization, wherein the additional scale-dependence caused by the loops is folded into the coupling, making it scale dependent. This makes clear two important facts: (A) the running of a coupling is purely a quantum phenomenon, due to higher-order loop diagrams contributing to the force magnitude; (B) the choice to fold the additional scale dependence into the coupling is a matter of convenience and preference.²

In quantum electrodynamics (QED), vacuum polarization is the only effect that (Fig. 3a-upper graph) causes the coupling to run. In QCD, more processes contribute: vacuum polarization (Fig. 3a-lower graphs), quark self-energy (Fig. 3b), vertex corrections (Fig. 3c), and other gluon loop corrections to the three-gluon and four-gluon vertices. How the relevant amplitude is separated into different graphs is conventional. For instance, the quark self-energy, Fig. 3b, does not contribute in the Landau gauge. Hence, stating which graphs contribute is partly arbitrary. In fact, one can even arrange and combine graphs so that α_s 's running is due only to gluon vacuum polarization, as in QED [3, 4].

¹When considering processes that involve spacelike momenta, we will use $Q^2 = -q^2 > 0$.

²In fact, this choice is not always made. One traditionally publishes experimental lepton scattering data corrected so that they are expressed in the Born approximation. This entails performing *radiative corrections* [2] that include the loops that makes α to run. Therefore, the classical coupling *constant* value, $\alpha \approx 1/137$, is used in the calculations to extract results from lepton scattering experiments rather than the running coupling.

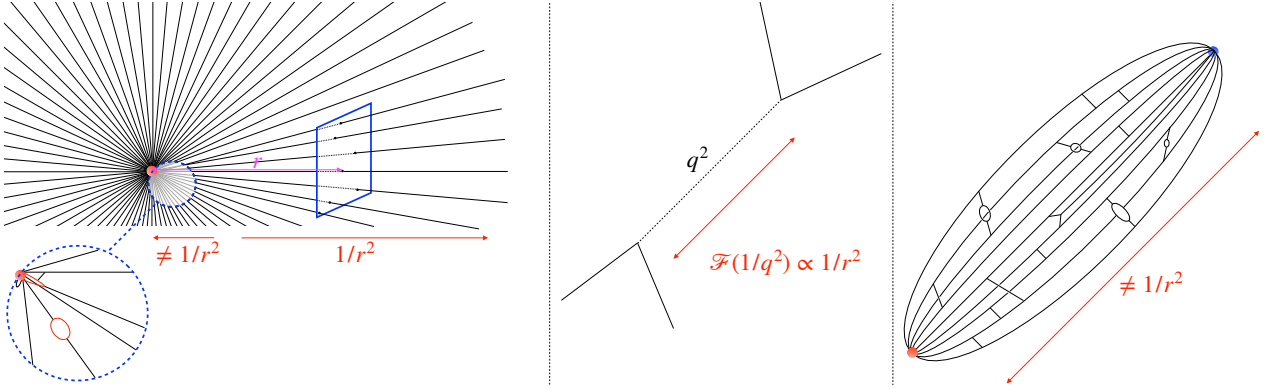


Fig. 2: **The inverse square law of forces, and where it fails.** For static sources, a classical force follows $\vec{F} = \frac{\mathcal{A}c_1c_2}{r^2} e^{-m|\vec{r}|} (1 + m|\vec{r}|)\vec{u}_r$, where \mathcal{A} is the force coupling, c_1 and c_2 are the source charges (masses for gravity, electric charge for electricity, color for QCD, and weak isospin for the weak force), \vec{r} is the vector linking the two sources, $\vec{u}_r \equiv \vec{r}/|\vec{r}|$, and m is the field mass, set to $m = 0$ in this chapter. Classically, the inverse square law, *i.e.* the $1/r^2$ factor, stems from the force flux that freely spreads in 3D space (left panel). The straight black lines are the field lines, the blue square represents the unit area, distant from the source by r , through which the flux is measured. The force equals the flux going through the area. The red sphere symbolizes one of the sources (the other is the test particle and therefore not shown). In QFT, the $1/r^2$ dependence originates from the Fourier transform of the gauge boson propagator (dashed line in middle panel) in the Born approximation; $1/r^2 \propto \mathcal{F}(1/q^2) \propto 1/r^2$ with q the boson 4-momentum. The $1/r^2$ law fails at short distances because of additional r -dependences from quantum loops, as illustrated in the magnified area in the left panel. The straight lines now depict the trajectories of the gauge bosons rather than field lines. Fermion loops are shown in red. The $1/r^2$ law also fails for strongly interacting non-linear theories because the self-interaction of the field prevents its free spreading (*viz* propagation) in space. QCD is the prototypical example of such phenomenon (right panel). In the renormalization process, the additional scale dependence from quantum loops is folded into the definition of the coupling rather than modifying the gauge boson propagator, thereby making the coupling scale-dependent. This is the origin of its running.

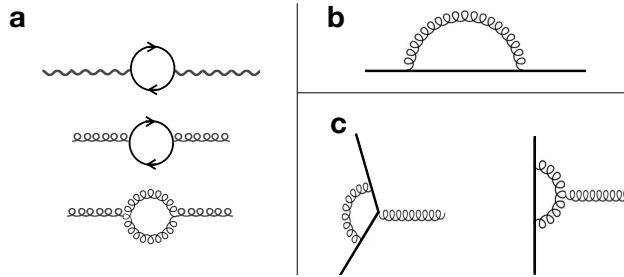


Fig. 3: **Short distance QED (panel a-top graph) and QCD (all panels) processes making α and α_s to run.** (a): Vacuum polarizations; (b): quark self-energy; (c): Vertex corrections. Other graphs exist, see [5] for the list up to next-to-leading order (NLO).

How loops alter the $1/r^2$ law is sketched in Fig. 4 (left: QED, right: QCD). For QED, pairs of virtual electron-positron temporarily appear around the bare charge, here that of an electron. The positrons are preferably closer to the bare charge because of their own opposite charge, while the virtual electrons tend to be farther. The total charge (bare+virtual) in a sphere of radius r is thus smaller than the bare charge. By Gauss's law, the total charge controls the magnitude of the coupling, so a *charge screening* appears: α decreases as r increases, asymptotically tending toward its long-range value $\sim 1/137$. For QCD, the charge-screening process is reversed because gluons carry colors. As depicted in Fig. 4, an emitted gluon carries away the initial color of the bare source, thereby spatially spreading the initial color charge. In Fig. 4, the bare quark is initially red but, eventually, is mostly green. Thus, it is transparent to high-resolution (relevant to large Q^2 processes) anti-red gluons, but not to lower-resolution (low Q^2) anti-red gluons that would amalgamate the bare quark and the gluon(s) that carried away its red color. Hence, α_s decreases with r , opposite to QED. Screening from quark+antiquark loops occurs in QCD but the spacial spreading of color (*anti-screening*) from gluon loops dominates. Were more types of quarks to exist, *i.e.*, were the number of flavors n_f larger in nature, screening would prevail once $n_f \geq 17$, and α_s would behave like QED's α . Vertex correction (Fig. 3c) further enhances the color spatial spreading, while quark self-energy (Fig. 3b) either screens the charge or leaves it unaffected, depending on gauge choice.

Coupling of theories without intrinsic scales, like QED or QCD, runs logarithmically. Quarks, electrons, gluons and photons are pointlike and massless³ so the momentum transfer in the reaction, Q^2 , is the only available scale. Therefore, the infinitesimal scale dependence of a

³Or nearly so for most of the fermions. The heavy quark masses can be considered infinite compared to the energy scale, and QCD remains without intrinsic scale.

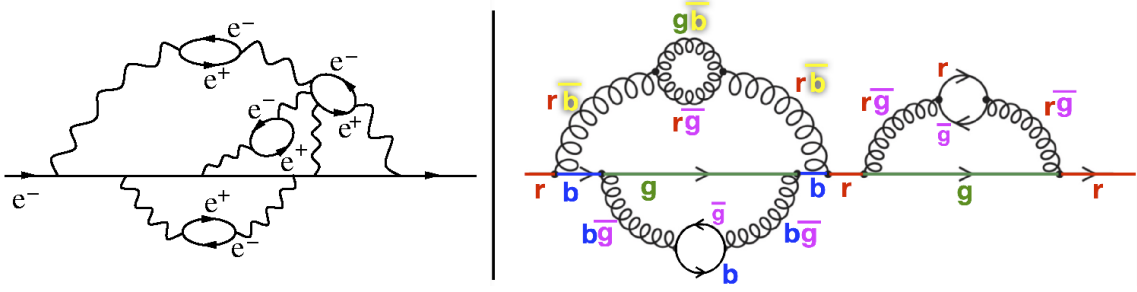


Fig. 4: **Left: screening of the QED electric charge by quantum loops.** Positrons tend to be nearer to the bare negative charge (horizontal line) than electrons. **Right: anti-screening of QCD color charges.** The color-charged gluons spatially spread the color initially carried by the quark: the initially red quark changes first into a blue quark when its red color is carried away by a gluon. Then, the quark becomes green after another gluon emission, etc. (Anti-blue is symbolized by yellow, and anti-green by magenta.) The spatial dilution of the initial red charge suppresses interaction *via* high-resolution anti-red gluons, while lower-resolution gluons still couple since they do not resolve the quark from the gluons carrying away the color. Thus, α_s grows weaker at shorter distances. (Figure from Ref. [6].)

coupling \gtrsim can only be:

$$\frac{d\gtrsim(Q^2)}{dQ^2} = \frac{f(\gtrsim)}{Q^2} = \frac{a_0 + a_1 \gtrsim + a_2 \gtrsim^2 + \dots O(\gtrsim^n)}{Q^2}, \quad (1)$$

where we assumed \gtrsim to be small enough so that any function of it can be expanded. The (dimensionless) expansion coefficients a_i are determined by the theory, see Section 1.3 for QCD. In fact, one can already infer that for QCD, $a_0 = a_1 = 0$, since for positive a_0 or a_1 , α_s would increase at large Q^2 , contradicting asymptotic freedom. And if a_0 or a_1 were negative, α_s would be unphysical (negative). Thus, for large Q^2 where $\alpha_s \ll 1$, a_2 dominates:

$$\alpha_s(Q^2) = \frac{-1}{a_2 \ln(Q^2/C)} \quad (2)$$

where C is an integration constant and $a_2 < 0$ fulfills asymptotic freedom. As Q^2 decreases, α_s increases and higher order $\ln^n(Q^2)$ terms become important. However, this description must ultimately break down when either **(A)** α_s becomes too large for Eq. (1) to be valid, or **(B)** when Q^{-1} reaches a value commensurate with the hadron size. Indeed, since confinement suppresses wavefunctions of colored particles when their wavelengths reach hadronic size, the very quantum effects responsible for the evolution of α_s are suppressed, making α_s constant there [7–11]. Clearly, conditions **(A)** and **(B)** are related since it is at the scale where α_s becomes large that the onset of confinement occurs, which in turn sets the hadron size.

The techniques used to compute α_s in the short and long distance regimes are quite different. Therefore, we discuss them separately in Sections 1.3 and 1.5. The large Q^2 (short-distance) regime is called the *ultraviolet* (UV) regime, and the low Q^2 (long-distance) one, the *infrared* (IR) regime. As of 2024, α_s is measured over 10 orders of magnitude in Q^2 : $4 \times 10^{-4} < Q^2/\text{GeV}^2 < 4 \times 10^6$ [1, 12].

A popular level account of α_s and its history is available in [13]. To go deeper than the present chapter, several reviews on α_s are available; *e.g.*, Refs. [6, 14–23]. The standard review for α_s in the UV is from the Particle Data Group (PDG) [14]. Most reviews cover only the UV domain. Some also discussing the IR domain are [6, 15, 20, 23].

1.3 Behavior of α_s at high-energy

The previous phenomenological description is formalized by the *renormalization* procedure. In an interacting theory, the strength with which a field (*e.g.*, the force field) couples to another (*e.g.*, itself or a matter field) is set by the coupling constant. Its value becomes dependent on the *arbitrary* UV cut-off (or other methods) that regularizes the UV-divergent integrals. This unphysical feature is removed by making the coupling scale-dependent (to *run*) and by anchoring the running to a value phenomenologically determined at a chosen scale. The *coupling constant* becomes a running *effective coupling*.⁴ How the coupling runs is determined by requiring physics to be independent of human conventions, here the choice of renormalization scheme (RS). The symmetry group resulting from this invariance, the renormalization group (RG), allows to compute the coupling behavior *via* group theory techniques. To see how, let us expand an observable R :

$$R(Q^2) = \sum_n r_n [\alpha_s(Q^2)]^n. \quad (3)$$

⁴The procedure makes the coupling to lose its classical status of observable: it now depends on the chosen RS and, possibly, on the gauge choice, etc. Definitions that maintain observability exist, *e.g.*, Section 1.6.

While R is RS-independent,⁵ the series elements r_n and α_s depend on the RS choice, except for r_0 and r_1 that are RS-independent. For r_0 , the reason is asymptotic freedom, $R \xrightarrow[Q^2 \rightarrow \infty]{} r_0$, and r_0 is an observable quantity, independent of RS. For r_1 , it is because at LO, α_s (Eq. (21) below) is RS-independent since, although α_s may not be observable, its running arises from physical processes and can thus be expanded with another coupling α'_s obtained in a different RS:

$$\alpha'_s = \alpha_s + v_2 \alpha_s^2 + v_3 \alpha_s^3 + \dots \quad (4)$$

Then, using the other scheme, $R(Q^2) = \sum_n r'_n [\alpha'_s(Q^2)]^n$ and Eq. (4) shows that r_1 is RS-independent.

QED's α slight RS-dependence makes it essentially constant in the IR [24], allowing us to take it as an observable measurable in the IR. This is not so in pQCD: α_s is highly RS-dependent [25] and perhaps may not exist in the IR where quarks and gluons degrees of freedom are occluded. Therefore, α_s is often taken as an intermediate quantity having at best a qualitative physical meaning. For instance, $\alpha_s^{\text{MOM}}(Q^2=1 \text{ GeV}^2) \simeq 1.5$ in the MOM RS [26, 27], about 3 times larger than in the $\overline{\text{MS}}$ RS [28], $\alpha_s^{\overline{\text{MS}}}(1 \text{ GeV}^2) \simeq 0.5$. This shows that α_s cannot quantitatively stipulate the actual strength of QCD. Yet, asymptotic freedom implies that the RS-dependence vanishes in the deep UV regime (the $R \xrightarrow[Q^2 \rightarrow \infty]{} r_0$ above), and then, the physical and intuitive meaning of α_s is approximately restored there. Furthermore, we will see in Section 1.5 that α_s can be defined so that it retains its observable character and phenomenological meaning.

Considerations on interpretation/RS-dependence aside, the running of α_s is well understood in the UV thanks to pQCD. Yet, the latter provides only the Q^2 -behavior, and experiments and lattice gauge theory (LGT) are deploying large efforts to determine the absolute magnitude of α_s . This must go hand-to-hand with advances in pQCD because α_s not being an observable, high-order pQCD series are needed to accurately extract α_s from actual observables. The importance of such endeavors is clear considering that, as said earlier, α_s is by far the least known of the four fundamental couplings. Also, comparing of α_s values obtained from distinct observables and at different Q^2 fundamentally tests QCD's internal consistency, and is thus a possible window into physics beyond the Standard Model. So, despite the well-known theoretical footing, α_s studies in the UV remain crucial. Let us now summarize the formalism providing the running of α_s .

The QCD Lagrangian density [29] is⁶:

$$\mathcal{L}_{\text{QCD}} = \sum_f \bar{\psi}_i^{(f)} (i\gamma_\mu D_{ij}^\mu - m_q \delta_{ij}) \psi_j^{(f)} - \frac{1}{4} F_a^{\mu\nu} F_{\mu\nu}^a, \quad (5)$$

where $\psi^{(f)}$ is the field for a quark of flavor f and bare mass m_q , $D_{ij}^\mu \equiv \partial^\mu \delta_{ij} + i\sqrt{4\pi\bar{\alpha}_s} t_{ij}^a A_a^\mu$, with $\bar{\alpha}_s \equiv \bar{g}^2/4\pi$ the bare coupling constant, t_{ij}^a the SU(3) generators, $a = 1, \dots, 8$ the color indices and A_a^μ the gluon fields, and $F_a^{\mu\nu} \equiv \partial^\mu A_a^\nu - \partial^\nu A_a^\mu + \sqrt{4\pi\bar{\alpha}_s} f_{abc} A_b^\mu A_c^\nu$, with f_{abc} the SU(3) structure constants. We can generally take $m_q \simeq 0$ (light quarks) and $m_q \rightarrow \infty$ (heavy quarks) compared to Q or the emerging QCD scale Λ_s (Eq. (22)). Then, Eq. (5) has no energy scale and defines a *conformally invariant* classical theory. Yet, phenomenologically, most QCD processes depend on Q , the process' 4-momentum flow. Therefore, a second scale must emerge at quantum level to normalize Q , thereby providing a dimensionless ratio. A ready candidate emerges from the renormalization procedure: the *regularization scale* or *subtraction point* μ . Its emergence in a classically conformal theory is called *dimensional transmutation* [30] and exemplifies a quantum anomaly, *viz* the breaking by quantum effects of a symmetry in the classical theory, here conformal symmetry. In other words, QCD does not carry all the properties of its classical version embodied by \mathcal{L}_{QCD} . The meaning of μ varies with the choices of regularization method and RS [6] which, together with the fact that the value for μ is chosen arbitrarily, implies that any observable must be independent of μ . For example, consider a dimensionless observable R that depends on the kinematic variables Q^2 and \mathbf{y} . The latter can be chosen to be dimensionless since they characterize a system without intrinsic physical scale. Expanding R in $\bar{\alpha}_s$,

$$R(Q^2, \mathbf{y}) = \sum_{n=0} r_n(Q^2/\mu^2, \mathbf{y}) \bar{\alpha}_s^n, \quad (6)$$

where the r_n are calculated perturbatively. For $n \geq 2$, divergences occur which, once regularized, depend on Q^2/μ^2 (rather than Q^2 , since there are no intrinsic scales). As explained in Section 1.2, the emerging scale dependence is assigned to the coupling $\bar{\alpha}_s$, apart from the classical $\propto 1/Q^2$ dependence. Thus, α_s acquires a running, and the pQCD series becomes:

$$R(Q^2, \mathbf{y}) = \sum_{n=0} r_n(\mathbf{y}, \alpha_s) \alpha_s^n (Q^2/\mu^2). \quad (7)$$

The chain rule applied on the μ^2 -independent of R yields

$$\frac{dR(Q^2, \mathbf{y})}{d\mu^2} = \left(\frac{\partial}{\partial \mu^2} + \frac{\partial \alpha_s}{\partial \mu^2} \frac{\partial}{\partial \alpha_s} + \frac{\partial Q^2}{\partial \mu^2} \frac{\partial}{\partial Q^2} + \sum_i \frac{\partial y_i}{\partial \mu^2} \frac{\partial}{\partial y_i} \right) R = 0. \quad (8)$$

⁵In practice, Eq. (3) is truncated to finite order so the perturbative approximant of R has a residual RS-dependence.

⁶We ignore gauge-fixing ghost fields since they are not fundamental nor required for our discussion.

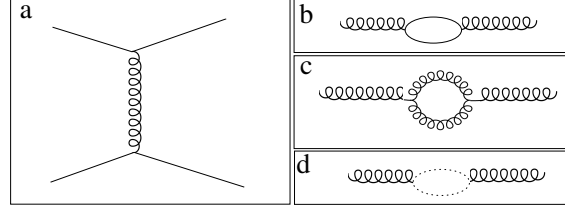


Fig. 5: Panel (a): 1st order quark–quark scattering: classical result (no quantum loops) leading to the $1/r^2$ law. Panels (b), (c) and (d): gluon propagator with a quark, gluon and ghost loops, respectively. (Figure from Ref. [6].)

Since \mathbf{y} and Q^2 are physical quantities (kinematic variables), $\partial Q^2/\partial\mu^2 = 0 = \partial y_i/\partial\mu^2$. Then, multiplying Eq. (8) by μ^2 and using only the Q^2/μ^2 ratio upon which α_s solely depends, yields the Renormalization Group Equation⁷ (RGE) [24, 31–34]:

$$\left(-\frac{\partial}{\partial[\ln(Q^2/\mu^2)]} + \beta(\alpha_s)\frac{\partial}{\partial\alpha_s}\right)R = 0, \quad \beta(\alpha_s) \equiv \mu^2\frac{\partial\alpha_s}{\partial\mu^2}, \quad (9)$$

which defines the “ β -function” that governs the running of α_s .⁸ Eqs. (8-9) hold in any domain, both UV and IR. The β -function can be expanded in the UV as:

$$\beta(\alpha_s) = -\frac{\alpha_s^2}{4\pi} \sum_{n=0} \left(\frac{\alpha_s}{4\pi}\right)^n \beta_n. \quad (10)$$

The β_n are computed perturbatively and are presently available up to $n = 3$ in several RSs, see [20] for their expressions, and to $n = 4$ in the $\overline{\text{MS}}$ RS, see [6]. (We remind that because the RS-dependence of α_s vanishes in the UV, β_0 and β_1 are RS-independent when the m_q are ignored.) In the jargon, α_s calculated up to β_n is said to be at the “ $n+1$ -loop” level since $n+1$ reflects the number of loops in the Feynman graphs of corresponding order. By their definition in Eq. (10), the β_n are independent of α_s . Instead, they are expansions in \hbar . They depend solely on the number of active quark flavors, n_f , *i.e.*, quarks whose mass $m_q \ll \mu$ allows them to enter the loops making α_s to run. As we will compute below, $\beta(\alpha_s) < 0$ in the UV and for physical n_f values. Then, from Eq. (9), $\alpha_s \xrightarrow{\mu \rightarrow \infty} 0$, *viz* asymptotic freedom. This finding [35, 36] was pivotal for understanding the strong force: the vanishing of α_s makes perturbation theory applicable in the UV, which led to establishing QCD as the QFT of the strong force, thereby completing the Standard model of particle physics [37]. This watershed in research on the strong force and particle physics was recognized by awarding the 2004 physics Nobel prize to the discoverers that in QCD⁹, $\beta_0 > 0$, and thus $\beta(\alpha_s) < 0$ in the UV [35, 36]. In the jargon, $\alpha_s \xrightarrow{\mu \rightarrow \infty} 0$ constitutes a *Gaussian fixed point* [41]. We will see in Section 1.5 that α_s also has a fixed point in the IR.

Let us now calculate the first-order (1-loop) β -function coefficient, β_0 . This will expose what phenomena make α_s to run. We provide here the direct calculation, using Feynman rules with amplitudes already regularized and renormalized in $\overline{\text{MS}}$, with $m_q = 0$. Another calculation method for β_0 , pedagogically reported in [6] and summarized in Section 1.8, employs renormalization constants and is useful to consult since it makes explicit the connection between running and renormalization. The LO quark-quark interaction is drawn in Fig. 5a. As it has no loops, it is classical, yielding the $1/r^2$ law from the Fourier transform of $1/Q^2$ in the gluon propagator. Quantum effects arise from loops attached to the propagators or vertices of the LO diagram. As explained earlier, the extra Q^2 -dependence they induce is folded into the coupling, making it run. The Feynman rules yield, for the gluon propagator with a quark loop (Fig. 5b):

$$D_q^{\mu\nu}(q) = -\frac{\overline{\alpha_s}}{3\pi} (q^\mu q^\nu - \eta^{\mu\nu} q^2) \ln(Q^2/\mu^2) n_f \frac{\delta_{ab}}{2}, \quad (11)$$

where $\eta^{\mu\nu}$ is the metric tensor, and a, b are the in- and out-gluon color indices. The gluon loop (Fig. 5c) adds a term:

$$D_g^{\mu\nu}(q) = \frac{\overline{\alpha_s}}{4\pi} N_c \delta_{ab} \left[\frac{11}{6} q^\mu q^\nu - \frac{19}{12} \eta^{\mu\nu} q^2 + \frac{1-\xi}{2} (q^\mu q^\nu - \eta^{\mu\nu} q^2) \right] \ln(Q^2/\mu^2), \quad (12)$$

with ξ a gauge-fixing term and $N_c = 3$, the number of colors. A longitudinal component is now present in the gluon propagator: $D_q^{\mu\nu} + D_g^{\mu\nu} \not\propto (q^\mu q^\nu - \eta^{\mu\nu} q^2)$, which violates current conservation: $(D_q^{\mu\nu} + D_g^{\mu\nu})q_\mu \neq 0$. There are several ways to fix this [6]. The most common is to introduce Faddeev-Popov ghosts [42], artificial¹⁰ particles designed so that their loop contribution (Fig. 5d),

$$D_{gh}^{\mu\nu}(q) = -\frac{\overline{\alpha_s}}{4\pi} N_c \delta_{ab} \left[\frac{1}{6} q^\mu q^\nu + \frac{1}{12} \eta^{\mu\nu} q^2 \right] \ln(Q^2/\mu^2), \quad (13)$$

cancel the longitudinal gluons, making the gluon propagator ($D_q^{\mu\nu} + D_g^{\mu\nu} + D_{gh}^{\mu\nu}$) purely transverse.

⁷Also called the Callan–Symanzik relation, Gell-Mann–Low relation or ’t Hooft–Weinberg relation, depending on the context and RS.

⁸We ignored the quark masses: $m_q \approx 0$ (light quarks) or $m_q \rightarrow \infty$ (heavy quarks). See [6] for a discussion on their second-order effect.

⁹That $\beta(\alpha_s)$ can be negative has a rich history. Before the possibility percolated to QCD, Vanyashin and Terentyev [38], and Khriplovich [39] discovered it for a SU(2) theory. G. ’t Hooft established it for an arbitrary gauge but reported his finding in his Ph.D. dissertation rather than in a journal [40].

¹⁰Ghosts are spin-0 fields that nevertheless obey Fermi-Dirac statistics.

In QCD, fermion self-energy (Fig. 3b) and vertex corrections (Fig. 3c) can affect the running of the coupling, contrary to QED where they cancel each other through the Ward identity [43, 44]. In $\overline{\text{MS}}$, self-energy and vertex corrections are, respectively:

$$G_q(p) = \frac{\not{p}}{p^2} \delta_{ab} \left[1 - \xi \frac{\overline{\alpha}_s}{4\pi} \frac{N_c^2 - 1}{2N_c} \ln(-p^2/\mu^2) \right], \quad (14)$$

$$\Gamma_\mu^{\alpha\beta;a}(q) = -i \sqrt{4\pi\overline{\alpha}_s} \frac{\lambda_{\alpha\beta}^a}{2} \gamma_\mu \left[1 - \frac{\overline{\alpha}_s}{4\pi} \ln(Q^2/\mu^2) \left\{ \xi \frac{N_c^2 - 1}{2N_c} + N_c \left(1 - \frac{1 - \xi}{4} \right) \right\} \right], \quad (15)$$

with $\lambda_{\alpha\beta}^a$ the Gell-Mann matrices and α, β the color indices of the in- and out-quarks. An advantage of $\overline{\text{MS}}$ is that pQCD series coefficients, and so α_s too, are gauge-independent. Thus, ξ can be assigned a convenient value, *e.g.*, $\xi = 0$ (Landau gauge). Then, the sum of the amplitudes from the propagators, Eqs. (11)-(14), and vertex, Eq. (15), provides the NLO corrected quark–quark interaction amplitude:

$$\mathcal{M} = \mathcal{M}_{\text{Born}} \left[1 + \frac{\overline{\alpha}_s}{4\pi} \left\{ \frac{2n_f}{3} - \frac{13N_c}{6} - \frac{3N_c}{2} \right\} \ln(Q^2/\mu^2) \right], \quad (16)$$

with $\mathcal{M}_{\text{Born}}$ the LO (classical) amplitude, Fig. 5a. The quark loops contribute the “ $2n_f/3$ ” term, and the gluon and ghost loops contribute the “ $-13N_c/6$ ” term, of opposite sign. The vertex correction term “ $-3N_c/2$ ” also causing anti-screening. The quark self-energy correction does not contribute in $\overline{\text{MS}}$, or any gauge-dependent RS when the Landau gauge is chosen, as evident from Eq. (14). The next step is crucial: the quantum corrections in Eq. (16) are folded into the constant $\overline{\alpha}_s$, thereby forming a running effective coupling,

$$\alpha_s(Q^2) = \alpha_s(\mu^2) \left[1 + \frac{\alpha_s(\mu^2)}{4\pi} \frac{2n_f - 11N_c}{3} \ln(Q^2/\mu^2) \right], \quad (17)$$

which, for $\alpha_s(\mu^2) \ln(Q^2/\mu^2) \ll 1$, yields:

$$\frac{4\pi}{\alpha_s(Q^2)} = \frac{4\pi}{\alpha_s(\mu^2)} + \frac{11N_c - 2n_f}{3} \ln(Q^2/\mu^2). \quad (18)$$

After Q^2 -differentiation,

$$-4\pi \frac{d\alpha_s(Q^2)}{\alpha_s^2(Q^2)} = \frac{11N_c - 2n_f}{3} \frac{dQ^2}{Q^2}. \quad (19)$$

Recalling the definition of β and its expansion, Eq. (10), then:

$$\boxed{\beta_0 = \frac{11N_c - 2n_f}{3}}. \quad (20)$$

Importantly, for the physical values of N_c and n_f , $\beta_0 > 0$. The sign of β determines how α_s runs. With β_0 , the 1-loop contribution, dominating in the UV, $\beta < 0$ and α_s decreases, leading to QCD’s asymptotic freedom. Inspection [6] of the higher loop contributions shows that $\beta_1 > 0$ for $n_f \leq 8$, $\beta_2 > 0$ for $n_f \leq 5$, and $\beta_3 > 0$ always, *viz* α_s still decreases at moderate Q^2 .

Solving Eq. (18) determines α_s at LO:

$$\boxed{\alpha_s(Q^2) = \frac{4\pi}{\beta_0 \ln(Q^2/\Lambda_s^2)}}. \quad (21)$$

where

$$\Lambda_s^2 \equiv \mu^2 \exp\left(-\frac{4\pi}{\beta_0 \alpha_s(\mu^2)}\right). \quad (22)$$

Eq. (10) is solved exactly and analytically only at 1-loop. An exact solution at β_1 -order (2-loop) is known [45], but involves the Lambert function W_{-1} with is therefore non-analytical. At β_2 , or 3-loop, or higher orders, no exact solutions are known and approximate solutions are obtained using an iterative method which can be systematically applied to any order and currently provides solutions up to β_4 (5-loop) in $\overline{\text{MS}}$ [46]. The exact 2-loop solution and iterative higher-loop solutions are provided in [6, 20]. Finally, the definition of Λ_s , Eq. (22), is for LO and differs at higher orders, see, *e.g.*, [17] for its exact nonperturbative expression. Comparing estimates of α_s up to β_4 (see Fig. 3.2 of Ref. [6]) reveals that starting at 2-loop, the β -series converges quickly in the UV: the effect of $n \geq$ loops and approximations is about 5% at $Q^2 = 2 \text{ GeV}^2$, near the edge of the UV domain. However, the difference between 1-loop and the higher-order results is typically above 20% there.¹¹

Once Eq. (10) is solved at the desired order and with the needed β_i calculated, Λ_s remains the only unknown quantity. According to QCD and as verified experimentally, $\alpha_s(Q^2)$ in the UV is monotonic with Q^2 , so knowing either Λ_s or $\alpha_s(Q_{\text{ref}}^2)$ at a given Q_{ref}^2 value, usually

¹¹These numbers reflect the effects of loops, not an uncertainty in α_s , which is significantly smaller (below 1%). The truncation uncertainty is obtained by computing the N^{th} LO pQCD series of an observable using α_s at n -loop, and comparing it to the result at N^{th} -LO and $(n - 1)$ -loop. It provides the overall truncation uncertainty from both the pQCD series (α_s expansion) and the β series (\hbar expansion).

chosen as $Q_{\text{ref}}^2 = M_Z^2$, provides $\alpha_s(Q^2)$ anywhere on the UV domain. Therefore, a value for Λ_s can be provided in lieu of the absolute magnitude $\alpha_s(Q_{\text{ref}}^2)$. Both are phenomenological quantities to be determined experimentally. Alternatively, nonperturbative theoretical methods, *e.g.*, LGT, can deduce them from other accurately known phenomenological inputs, *e.g.*, the nucleon mass. In other words, Λ_s (or $\alpha_s(Q_{\text{ref}}^2)$) is neither determined nor explained within QCD, even nonperturbatively, just as $\alpha \approx 1/137$ is not explainable within QED.

The Landau pôle Λ_s determines the rate at which $\alpha_s(Q^2)$ changes with Q^2 . It also provides the scale where $\alpha_s^{\text{pQCD}} \rightarrow \infty$, where pQCD has clearly failed. This, however, is a qualitative rather than a fully objective indication: like α_s , Λ_s is typically not an observable. Beyond 2-loops, it is RS-dependent. It also depends on the loop order at which α_s is expanded and the method used to solve Eq. (10). Values for Λ_s in different RS typically range from 0.3 to 1 GeV; see Table 3.1 in Ref. [6], which also provides the all-order relation between Λ_s in different RS. The place where the pQCD expression of α_s diverges, exactly at $Q^2 = \Lambda_s^2$ at 1-loop (see Eq. (21)) and nearby for higher-order approximations, is called the Landau pôle [47, 48]. It was first encountered in QED, at $\Lambda_{\text{EM}} \sim 10^{30-40}$ GeV, well above the Planck scale and thus well within a domain where the Standard Model, and perhaps QFT, should be superseded by a more fundamental theory. Thus, the QED Landau pôle is irrelevant. Since α_s runs opposite to α , the QCD Landau pôle sits at low energy ($\Lambda_s \approx 0.5$ GeV) but is also irrelevant. The pôle just signals where the QFT perturbative treatment has failed since an observable's series expanded in α_s would “doubly” diverge because (A) each next order correction would typically grow larger, and (B) $\alpha_s \rightarrow \infty$. Such divergence is not observed.¹² Likewise, the β -function series is similarly affected (but not its β_n coefficients, which are expanded in \hbar). Despite the Landau pôle being unphysical, Λ_s is often called *confinement scale* because it lies within the nonperturbative regime where confinement – a nonperturbative phenomenon – occurs and because it suggests that there, α_s has become large enough to trigger the confinement process. The Landau pôle has sometimes been incorrectly considered as physically relevant. For instance, the QED Landau pôle challenged the adequacy of QFT¹³ as a description of nature [49]. As already mentioned, this worry vanishes once one realizes that QED is a low-energy effective theory, to be superseded at energies well below its Landau pôle. Another example is the Landau pôle being sometimes thought, in QCD's early days, as causing quark confinement. This was dubbed “IR slavery,” a pleasing but erroneous counterpart of UV's asymptotic freedom [50]. Nevertheless, within a specific theoretical framework, one may relate Λ_s to a physical scale, *e.g.*, that characterizing the hadron mass spectrum. This has been shown *via* lattice gauge theory (LGT) [17], the Dyson-Schwinger equations (DSE) [4], or holographic light-front QCD (HLFQCD) [51]. In the latter approach, the Landau pôle evolves from a real $Q^2 > 0$ pôle (therefore unphysical) to an imaginary pôle $i\Lambda_s$ in the complex Q^2 -plane, as the scale for hadron masses and confinement evolves from zero to its physical value [52], see Section 1.7 for details.

1.4 Methods of determinations of α_s at short distances

As mentioned, the absolute scale of α_s , or equivalently Λ_s , is not calculable within QCD. They are therefore obtained either experimentally or by relating them with nonperturbative techniques to other phenomenologically determined scales, like the nucleon mass. Observables providing α_s are numerous. Indeed, any hadronic observable with a pQCD expansion is usable. In practice, however, some observables are better suited for precision extractions of α_s . On the theory side, LGT is preferred as it is a well-controlled approximation to QCD unlike many models of hadron structure whose uncertainties are difficult to assess. Yet, some models have provided compelling determinations [4, 53]. Here, we briefly outline the methods to obtain α_s , giving examples of the most common observables that yield a precise α_s . More exhaustive lists are in the PDG review and compilation of α_s in the UV [1] and in the LGT-oriented review from the FLAG collaboration [17]. In both cases, the compiled results are in the $\overline{\text{MS}}$ RS (which reminds us that α_s is generally not an observable).

For $Q^2 \gg \Lambda_s^2$, the influence of Λ_s – and *a fortiori* that of light quark masses – must vanish. Furthermore, quarks being pointlike and asymptotically free, no structures exist at large Q^2 , and hence, no new scales arise. The appearance of a conformal behavior, known as *Bjorken scaling* [54, 55], implies a Q^2 -independence of hadronic structure quantities. Scaling violations at large Q^2 reflect the residual influence of Λ_s (and to a lesser extent, that of hadron masses and structures). This offers a first way to access Λ_s or α_s typified by charged lepton–quark scattering, Fig. 6A. The reaction is elastic, quarks being structureless, and occurs during deep inelastic scattering (DIS) of a lepton off a nucleon. At LO, scaling violations originate from the struck quark emitting a gluon, pair creation from that gluon, and photon–gluon “fusion” (photon–gluon interaction *via* quark pair creation). At NLO, quark self-energy and quark–photon vertex corrections also contribute. The ensuing Q^2 -dependence obeys the Dokshitzer–Gribov–Lipatov–Altarelli–Parisi (DGLAP) equations [56–59], which provide the formalism to extract α_s . In practice, the Q^2 -dependence of nucleon structure quantities is fit using DGLAP, together with parameterizations of the (nonperturbative) momentum distributions of the quarks and gluons in the nucleon (PDFs: parton distribution functions). Several collaborations use this extraction method, see [1, 6].

Observing hadronic jets is another way to access α_s *via* hard gluon emissions. For instance, Fig. 6B shows a 3-jet event where one jet developed from a hard gluon. The gluon emission probability, and thus also of $\gamma^* q \rightarrow qg$, being proportional to α_s , the 3-jet event rate normalized to the 2-jet rate directly provides α_s . The geometry of the particle collision outcomes can also provide α_s . Such geometry is analyzed with *event shape* observables, *e.g.*, the *thrust*, which quantifies the anisotropy of the particle emission produced in the collision, Fig. 6D. In the infinite momentum-transfer limit, all particles are aligned along a preferred axis, revealing the back-to-back produced $q\bar{q}$. At finite momentum-transfer, gluon emission from the quarks isotropizes the jet distribution geometry, with a spherical symmetry at low momentum-transfer. The deviation from anisotropy being due to gluon emissions, it allows access to α_s . Other event shape observables are

¹²Hadronic observables, *e.g.*, form factors and structure functions, have been measured over Q^2 domains that comprise Λ_s without showing any unusual behaviors such as divergences or discontinuities. The Landau pôle unphysical nature is evinced by other facts: the value of Λ_s depends on the (arbitrary) RS choice; and were the pôle genuine, it would produce particles of imaginary mass $m = q \equiv \sqrt{-Q^2} = i\Lambda_s$, *i.e.*, tachyons.

¹³The pôle famously steered L. Landau away from QFT and, through his ascendancy, most of Soviet research on particle physics.

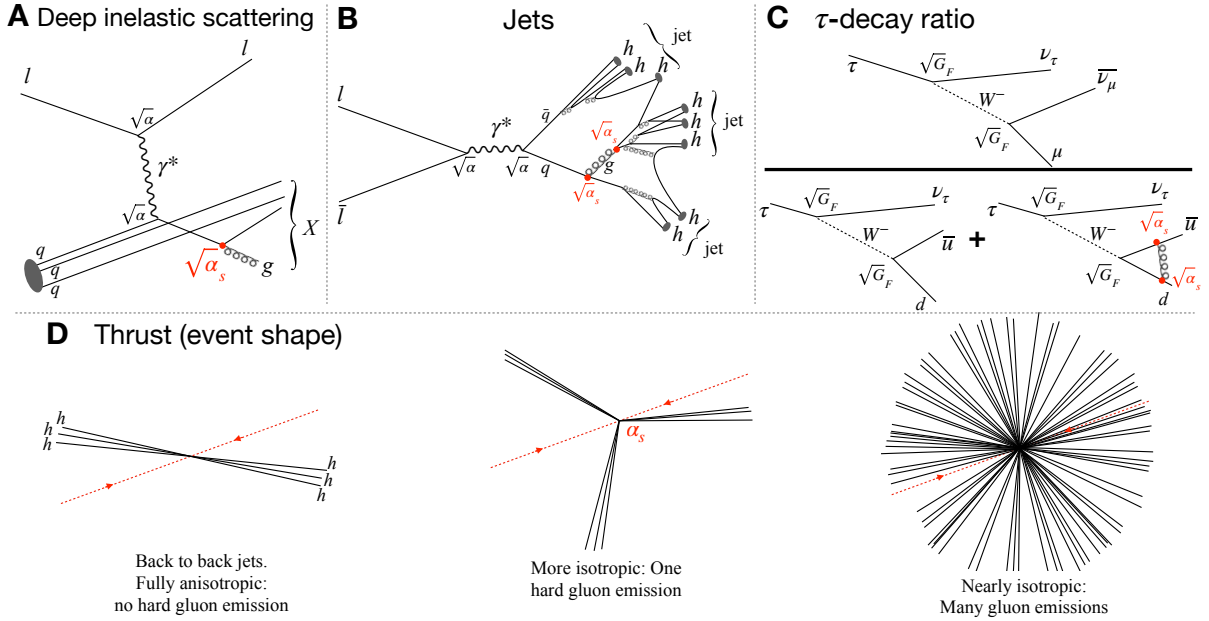


Fig. 6: **High-energy reactions typically used to determine α_s .** A curly line with a g label denotes the hard gluon that allows access to α_s . (“Hard” means a high-energy gluon emitted at large angle from its parent quark.) Softer gluons are shown by unlabelled curly lines. **A**: Deep inelastic scattering of a charged lepton l by a nucleon (grey blob). X denotes the undetected final hadronic state. **B**: Lepton-antilepton annihilation, eventually forming hadronic jets (h denotes a hadron). **C**: Comparison between leptonic and hadronic τ -decays. **D**: Geometrical variation of the jet distributions. The red dashed lines are the two colliding particles and the solid lines the produced hadrons.

used similarly. Also, inclusive cross-sections of heavy quark (bottom, top) production in collisions now accurately provide α_s , owing to refinements in theoretical understanding [6].

Other ways to access α_s are to compare the hadron production rate in $\bar{l}l$ annihilation to that of muons, or comparing hadronic to leptonic decay widths of a particle ($Z^0, W^\pm, \gamma^* \dots$) produced in the annihilation [60]. The sensitivity to α_s arises mostly through hard gluon emission by a quark or antiquark. The example of the ratio of τ -decay into hadrons over that of $\tau \rightarrow \nu_\tau e^- \bar{\nu}_e$ is sketched in Fig. 6C. It provides the most precise experimental extraction of $\alpha_s(M_Z)$ because evolving $\alpha_s(M_\tau)$ to $\alpha_s(M_Z)$ reduces its uncertainty by an order of magnitude.¹⁴ However, its rather low $Q^2 = M_\tau^2 = 3.16 \text{ GeV}^2$ value raises accuracy issues that remain debated [6, 60]. It causes non-trivial higher-order pQCD and nonperturbative QCD contributions. Furthermore, the produced ν_τ allows the W^- momentum to take any kinematically allowed values, including zero. Yet, a pQCD treatment is possible thanks to analyticity arguments. Several perturbative schemes are used for such analyses but the resulting α_s values are generally in tension. Which scheme is accurate and how to resolve the tension remains unclear [61–64]. In global averages of α_s from τ -decay, the difference between the various schemes is split and taken as an uncertainty.

Three types of uncertainties contribute in the experimental extraction of α_s : (A) experimental uncertainties; (B) truncation of the pQCD series to a finite order; and (C) possible nonperturbative contributions. Observables competitive in extracting α_s balance these contributions, often differently. The list also makes clear that improvement experimental precision data must be accompanied by theoretical advances in determining the observables’ pQCD series at sufficiently high order, and efforts to control the nonperturbative corrections.

Presently, the most accurate way to obtain α_s is LGT, with a precision of $\sim 0.7\%$ [17]. Ref. [20] provides an introduction to LGT in the context of determining α_s . The FLAG collaboration [17] compilation is the authority for $\alpha_s(M_Z)$ from LGT, and provides a comprehensive summary of the LGT methods. LGT accesses α_s like experiments do: an appropriate quantity¹⁵ is computed and matched to the corresponding pQCD series. Optimizing the match yields α_s . It results from the procedure that although LGT is a nonperturbative formalism, its α_s is RS-dependent, with the RS that of the pQCD series. As with experimental extractions, different quantities offer different advantages, and groups performing LGT calculations have selected different quantities. Currently, the best ones for $\alpha_s(M_Z)$ are Wilson loops, heavy-quark potential at short distances, heavy-quark current two-point functions, and α_s itself in association with the step-scaling method [65]. Other quantities are various QCD vertices, the Dirac operator, and vacuum polarization, but they are for now not as precise.

LGT is not the only nonperturbative method available for $\alpha_s(M_Z)$ computation, but it is currently the only one trusted by the PDG in its compilation [1]. Other methods providing precise determinations of $\alpha_s(M_Z)$ include the Dyson-Schwinger equations (DSE [66]) combined with LGT [67], and AdS/QCD [51, 68, 69].

¹⁴Specifically, $\delta\alpha_s(M_Z) = \left(\frac{\alpha_s^2(M_Z)}{\alpha_s^2(M_\tau)}\right) \delta\alpha_s(M_\tau) \approx 0.11 \delta\alpha_s(M_\tau)$ because $\left|\frac{d(1/\ln(Q^2/\Lambda_s^2))}{dQ^2}\right| = \frac{1}{\ln^2(Q^2/\Lambda_s^2)}$.

¹⁵For LGT, the quantity need not be an observable, unlike for experiments.

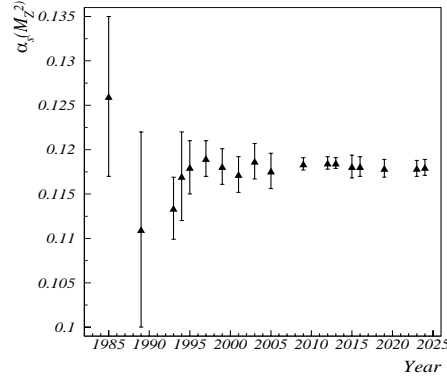


Fig. 7: **History of the global average of $\alpha_s(M_Z)$** (data from the Particle Data Group). The notable improvement after 1989 reflects the impact of CERN’s LEP (e^+e^- collisions) and DESY’s HERA ($e^{+/-}p$ collisions) starting operations, together with theoretical advances on NNLO calculations. Next, in the mid-2000s, LGT determinations came to dominate the global average, albeit in 2015, the uncertainty was revised upward as it was assessed that they were larger than initially estimated. Then, the steady decrease in uncertainty resumed, with presently $\alpha_s(M_Z) = 0.1180(9)$.

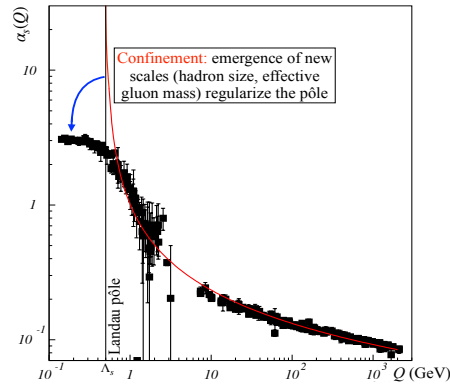


Fig. 8: **Regularization of the Landau pole.**

We conclude this section with the historical progress and perspectives in determining $\alpha_s(M_Z)$. Past and present PDG global averages are shown in Fig. 7. Currently, $\alpha_s(M_Z) = 0.1180 \pm 0.0009$ ($\overline{\text{MS}}$ RS) [1]. Accuracy will continue to improve as new data become available, as new facilities, *e.g.*, EIC [70, 71] or EicC [72, 73] come online or existing ones are upgraded, *e.g.*, LHC [74] or JLab [75]. As mentioned, for experimental extractions of $\alpha_s(M_Z)$ to reach their full potential, pQCD theoretical developments must go hand-in-hand.

1.5 Long distance behavior of α_s

So far we have discussed the UV domain of weakly-coupled QCD where α_s is most familiar thanks to pQCD’s power. Now, what happens outside the UV? pQCD “predicts” that α_s diverges when $Q^2 \rightarrow \Lambda_s^2$, see Section 1.3. This divergence is generic to couplings calculated perturbatively: we saw that it also occurs in QED. It merely signals the applicability limit of perturbation theory. Hence, color confinement cannot come from the Landau pole which would, anyway, generates unphysical tachyons. As already mentioned, no Landau pole is expected in reality for QED since it will be superseded by a more fundamental theory, nor for QCD because the Q^2 -dependence of the actual coupling is suppressed in the IR by the physical hadron size. This one imposes a maximum wavelength in the loops causing the running, thereby stopping it [7, 8, 11], Fig. 8. What happens to the pole is discussed in Section 1.7. The absence of Q^2 -dependence of α_s in the IR, *i.e.*, the vanishing QCD β -function, is variously named the *freezing* of α_s , the *conformal window* of QCD, or the $Q^2 = 0$ *fixed point*.

Nonperturbative studies of α_s are more arduous than those using pQCD. Yet, they are crucial because in nature, the strong force manifests itself mostly nonperturbatively. For example, almost all of the visible mass in the universe emerges from QCD IR dynamics¹⁶ [76], with unsurprisingly the IR behavior of α_s being crucial to the process [8, 9, 51]. Another important example is dynamical chiral symmetry breaking, to which magnitude of α_s in the IR is directly [10, 77–79]. The chief reason why IR studies of α_s are difficult is its various possible definitions, without one seemingly superior to the others. This contrasts with pQCD with its single agreed definition. The issue is largely due to having no definite nonperturbative solution of QCD, with many methods being tried. Should one method lead to a clear analytical nonperturbative solution of QCD, it would yield a compelling candidate for α_s . The picture just drawn may seem bleak but in an encouraging recent development, several nonperturbative methods, namely, LGT, DSE, and AdS/CFT, have produced IR couplings that

¹⁶The Higgs mechanism contributes at the few % level.

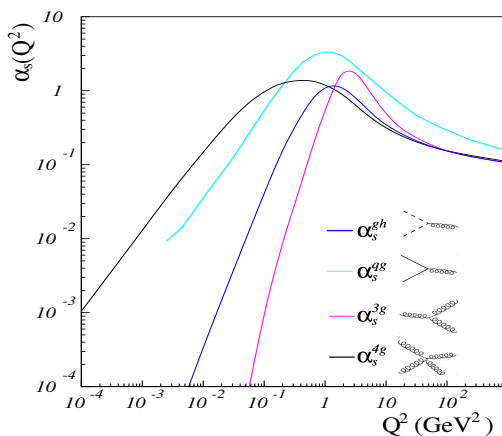


Fig. 9: **Vertex couplings for a renormalization scheme not fulfilling the Slavnov-Taylor Identities.** The ghost-gluon (α_s^{gh}), quark-gluon (α_s^{qg}), 3-gluon (α_s^{3g}), and 4-gluon (α_s^{4g}) couplings behave very differently, except in the UV where the STI always hold. Calculations are from Refs. [84, 85] (Landau gauge, MOM RS). In formalisms enforcing the STI, a unique coupling characterizes the vertices: $\alpha_s(Q^2) = \alpha_s^{gh}(Q^2) = \alpha_s^{qg}(Q^2) = \alpha_s^{3g}(Q^2) = \alpha_s^{4g}(Q^2)$, $\forall Q^2$. Figure adapted from Fig. 4.3 of [6], see this reference for details.

are consistent and also agree with IR experimental data on α_s . This offers a compelling case for having finally identified a canonical IR definition for α_s . In this Section, we discuss the origin of the aforementioned challenges and then describe the recent developments.

As just said, studying $\alpha_s(Q^2)$ in the IR is challenging chiefly because no obvious definition of α_s is available. (Remember, α_s need not be an observable, see Section 1.3). Other reasons are **(A)** systematics or model bias in nonperturbative calculations are often hard to control; **(B)** the RS-dependence increases at lower Q^2 ; and **(C)** the various vertices (3-gluon, 4-gluon, quark-gluon, or ghost-gluon) may have different couplings, see Fig. 9. That is, distinct magnitudes and Q^2 -dependence may characterize these vertices.¹⁷ This occurs when the chosen gauge and RS conculcate the Slavnov-Taylor identities (STI) [80, 81], QCD's version of QED's Ward identity [43, 44]. For instance, in the Landau gauge and MOM RS, the various vertices couplings behave quite differently (Fig. 9). In the $\overline{\text{MS}}$ RS, the STI hold, so the vertices couple consistently. Unfortunately $\overline{\text{MS}}$ is not suited to most nonperturbative methods. Clearly, to characterizes QCD's strength, we need a formalism that respects the STI, or at least, in which all vertex couplings are equal and gauge-independent. A solution is to define α_s as an observable following QED's procedure for α [82]. Such a definition is available [83] and will play a central rôle in this Chapter.

Historically, many IR definitions of α_s have been used, producing **(A)** a range of values for $\alpha_s(Q^2 \sim 0)$ from 0 to ∞ [20], and **(B)** much confusion. All major nonperturbative approaches to QCD have been solicited¹⁸, namely LGT, DSE [66] and AdS/QCD [68], as well as many models. The different approximations underlying these methods¹⁹ or the fact that the models are not explicitly rooted in QCD is one reason why their predictions differed so much. Other reasons were the differences in the basic definition of α_s ; the choice of vertex to compute α_s with methods/RS not fulfilling the STI; the choice of gauge and RS; and/or the appearance of multiple solutions to the same equations, providing differing α_s .²⁰ Now, the major nonperturbative methods have converged toward a meaningful definition of α_s that encompasses IR phenomena [6, 20]. Before discussing this advance, we will first briefly present the quest for such a definition, mentioning only pioneering attempts and glossing over subsequent important works by many, who studied and refined these attempts.

J. M. Cornwall, in an influential pioneering work [89], developed the *pinch technique* to calculate using the DSE a gauge-independent α_s that freezes in the IR. While IR-freezing had been already conjectured at the advent of QCD [90–92], it was by no means the only behavior envisioned. Other proposals were that α_s vanishes as $Q^2 \rightarrow 0$ [88, 93], that it diverges as $1/Q^2$ [94] (based on considering the $Q\text{-}\bar{Q}$ static quark potential), or that it monotonically rises with $1/Q^2$ without diverging [95]. The α_s definition used by Cornwall relies on correlation functions (specifically, the gluon propagator), a prevalent way to define α_s , see Section 1.8. Other notable definitions directly use phenomenology,²¹ the effective charge concept [83], or analytic approaches [95, 102], with the two latter making α_s an observable.

From these studies and developments emerged a fruitful definition of the IR coupling, the effective charge method [83, 110, 111]. It was computed [3] using the pinch technique [89] and the Background Field [112] method. The latter enforces gauge independence and the whole formalism obeys the STI. Then, QCD is characterized by a unique α_s , the same for all vertices. Importantly, and deviating from the original definition [83], this α_s is not defined with a specific process and therefore, is process-independent. It is obtained from correlation functions calculated with either the DSE or LGT [3, 4], see Section 1.8. The result is shown in Fig. 10 and agrees with the phenomenological

¹⁷This may seem odd, but it just means that the various quantum loops contribute differently to different vertices which, at classical level (bare coupling $\bar{\alpha}_s$) or observational level (deep UV limit, or defining α_s as an observable) do couple with a universal strength.

¹⁸Except for chiral effective field theory [86] because it uses hadronic degrees of freedom, which do not couple *via* α_s .

¹⁹*e.g.*, spacetime discretization in LGT or truncation prescriptions for the DSE.

²⁰Namely, the *scaling* [87] vs. *decoupling* [88] solutions: when α_s^{gh} is computed in the MOM RS the first leads to a freezing α_s^{gh} and the latter to a vanishing one. The recent consensus is that nature realizes the decoupling solution. This means that if a gauge requires ghost fields, the ghost stops interacting with the gluons in the IR. Thus, α_s^{gh} is not directly relevant to quantifying QCD's IR strength (albeit insightful regarding the interaction of ghosts with gluons). Fig. 9 shows decoupling solutions.

²¹For instance, using constituent quark models, the $Q\text{-}\bar{Q}$ potential, or the hadronic spectrum [94, 96–101].

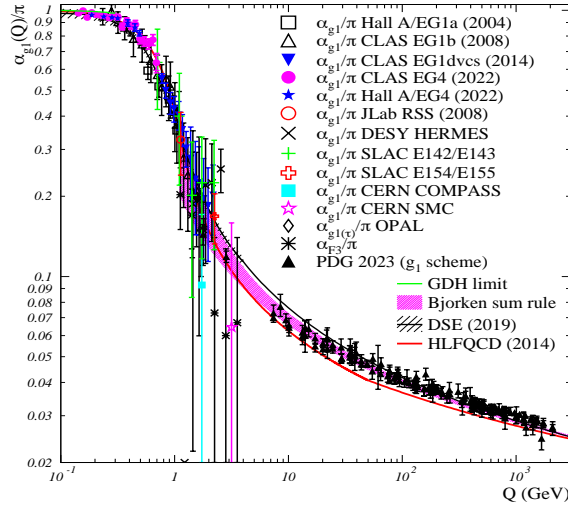


Fig. 10: **The QCD coupling at all scales.** The experimental data [12, 103, 104], shown by the symbols, are in the g_1 scheme, *viz* the effective charge definition (Section 1.6) applied to the Bjorken sum rule [105]. Exceptions are the OPAL datum extracted from τ -decay and converted to the g_1 scheme using the CSR [106], α_{F_3} obtained from the GLS sum rule [107] and expected to be nearly equal to α_{g_1} [20], and the PDG data [1], converted from $\overline{\text{MS}}$ to the g_1 scheme. The nonperturbative calculations are using the HLFQCD framework (Section 1.7), or the DSE formalism with lattice determinations of correlation functions (black-hatched band) (Section 1.8). The green line and magenta band are α_{g_1} deduced from, respectively, the GDH sum rule [108, 109] and the Bjorken sum rule + $\Lambda_s^{\overline{\text{MS}}}$ from the PDG. Other IR determinations of α_s exist, *e.g.*, [89] and [101]. When converted into the g_1 scheme [25], they agree with the data.

coupling [12, 103, 104] that follows the effective charge prescription [83] applied to the Bjorken sum rule [105]. It also agrees with α_s calculated using AdS/QCD [113], Section 1.7. In the next sections, we provide details on the central ingredients mentioned in this brief description, namely effective charges, the AdS/QCD calculation, and the DSE/LGT one. Other methods that have been used to study α_s in the IR are described in [6, 20, 23]

1.6 Effective charge method

QCD effective charges, devised by Grunberg [83, 110, 111], are defined so that pQCD series stop at first order in their coupling (\equiv effective charge) expansion. Thus, an effective charge encompasses all higher-order terms in the perturbative coupling α_s^{pQCD} : gluon emission, vertex corrections \dots that drive the higher-order DGLAP evolution. We illustrate the concept with the Bjorken sum rule [114–119]:

$$\Gamma_1^{\text{p-n}}(Q^2) \equiv \int_0^1 g_1^{\text{p-n}}(x, Q^2) dx = \frac{g_A}{6} \left[1 - \frac{\alpha_s^{\text{pQCD}}(Q^2)}{\pi} - 3.58 \left(\frac{\alpha_s^{\text{pQCD}}(Q^2)}{\pi} \right)^2 - 20.21 \left(\frac{\alpha_s^{\text{pQCD}}(Q^2)}{\pi} \right)^3 + \dots \right] + \sum_{n>1} \frac{\mu_{2n}(Q^2)}{Q^{2n-2}}, \quad (23)$$

with $g_1^{\text{p-n}}(x, Q^2)$ the isovector nucleon spin structure function, x the Bjorken scaling variable, g_A the nucleon axial charge and $\mu_{2n}(Q^2)$ are higher-twist coefficients. The series coefficients are in $\overline{\text{MS}}$ and for $n_f = 3$. The associated effective charge α_{g_1} is then defined by:

$$\Gamma_1^{\text{p-n}}(Q^2) \equiv \frac{g_A}{6} \left(1 - \frac{\alpha_{g_1}(Q^2)}{\pi} \right) \implies \alpha_{g_1}(Q^2) = \pi \left(1 - \frac{6}{g_A} \Gamma_1^{\text{p-n}}(Q^2) \right) \quad (24)$$

where the label g_1 in α_{g_1} indicates the observable defining the effective charge. Hence, both short distance (bracket in Eq. (23)) and long distance (μ_{2n}/Q^{2n-2} terms) effects became encapsulated in α_{g_1} . This generalizes the RGE procedure that makes the coupling *constant* to run by including quantum loop effects in it. Effective charges remain defined in the IR and are RS-independent since any pQCD approximant is RS-independent at LO (Section 1.3). In fact, they are observables, thus devoid of Landau pôle. In the UV, Eqs. (23-24) yield the relation between α_{g_1} and the standard pQCD coupling:

$$\alpha_{g_1}(Q^2) = \alpha_s^{\text{pQCD}}(Q^2) + 3.58 \frac{(\alpha_s^{\text{pQCD}}(Q^2))^2}{\pi} + 20.21 \frac{(\alpha_s^{\text{pQCD}}(Q^2))^3}{\pi^2} + \dots \quad \Big|_{\text{UV only}} \quad (25)$$

More generally, once an observable is chosen to define an effective charge, all other effective charges follow *via* commensurate scale relations (CSR) [106], thereby ensuring the predictive power of QCD.²² CSR also show that the choice of observable defining an effective charge is equivalent to a RS choice.

²²CSR are known in the UV domain. Extending them to the IR is discussed in Refs. [25, 51, 69, 106].

It is advantageous to define an effective charge with the Bjorken sum rule because its pQCD series is relatively simple and known to high order ($N^4\text{LO}$). Furthermore, g_A is well-known [1], $\Gamma_1^{p-n}(Q^2)$ is extensively measured and where measurements are lacking, reliable relations [108, 109, 114, 115] supplement them [6]. But most importantly, α_{g_1} is, to good approximation, interpretable as a standard coupling, including in the IR.²³ This is because Γ_1^{p-n} is an isovector integral in which coherent effects (i.e., involving rigidly linked quarks) are highly suppressed [6, 20, 120]. This is remarkable since in the IR, individual quarks cannot usually be isolated by the probing process, making a single quark's interaction inaccessible, while it is what is needed to measure the force magnitude. Fig. 10 shows α_{g_1} extracted from the world data on Γ_1^{p-n} [121–146].

1.7 Holographic Light-Front QCD

The AdS/QCD calculation of α_s is done with the HLFQCD model [53], an approach based on light-front (LF) canonical quantization, in which a field is quantized using LF time, $x^+ \equiv t + z$, (here, z is one of the 3 space coordinates) rather than the usual Galilean time t [147, 148]. This results in a Poincaré-invariant formalism, free of the pseudo-dynamics that complicates the usual canonical quantization based on t [149, 150]. LF quantization provides a rigorous nonperturbative approach to solving QCD, resulting, for $m_q \rightarrow 0$, in hadronic structures described by a relativistic Schrödinger equation [151]. The equation is solvable but the confining potential term has thus far been too difficult to compute ab-initio. Instead, gauge-gravity, or AdS/CFT, duality [152] is used. It posits that classical gravity in a $(n+1)\text{D}$ negatively curved spacetime (anti-de Sitter, AdS, spacetime) is dual to a conformal field theory (CFT) residing on the boundary of the $(n+1)\text{D}$ spacetime, i.e., in a $n\text{D}$ Minkowski (flat) spacetime. Crucially, for $m_q \rightarrow 0$, QCD's Lagrangian, Eq. (5), is that of a CFT. We saw in Section 1.3, that the classical conformal symmetry is broken by a quantum anomaly that manifests as a ~ 1 GeV phenomenological scale. Far enough from that scale, QCD is approximately conformal: deep-UV displays Bjorken scaling [54, 55], and a similar dearth of Q^2 -dependence is observed in the deep-IR: α_s freezes. Then, AdS/CFT applied to QCD yields AdS/QCD.²⁴ A semiclassical²⁵ potential for the relativistic Schrödinger equation can then be computed using generic symmetries of QCD for $m_q \rightarrow 0$. Several ways exist to do so, all leading to the same harmonic oscillator form, $U(\zeta) = \kappa^4 \zeta^2 + b$, where ζ is the transverse parton separation in LF coordinates, κ is the quantum anomaly's scale (therefore directly related to Λ_s [25, 51, 69]), and b depends on κ and the spin representations in AdS space. For $m_q = 0$, κ is universal. It can be deduced from any hadron masses, e.g., $\kappa = M_p/2$, with M_p the proton mass [53], or from Λ_s [52, 69]. To the $U(\zeta)$ in the LF theory corresponds a deformation of the AdS space given by a term $\exp(\kappa^2 z_h^2)$ factoring the AdS metric, with z_h being the 5th (“holographic”) coordinate of the AdS space. The factor $\exp(\kappa^2 z_h^2)$ breaks conformality and grows with z_h , causing confinement. Then, z_h is related to the CFT momentum scale [153]: $Q \sim 1/z_h$.

To calculate α_s in HLFQCD, one starts with the general relativity Action applied to AdS spacetime:

$$S = -\frac{1}{4} \int \sqrt{g} \frac{1}{\hat{a}^2} F^2 d^5 x, \quad (26)$$

where F is the field, \hat{a} its coupling and $g \equiv \det(g_{\mu\nu})$. $g_{\mu\nu}$ is the AdS metric of invariant interval $ds^2 = \frac{R^2}{z_h^2} (\eta_{\mu\nu} dx^\mu dx^\nu - dz_h^2)$, with R the AdS radius and $\eta_{\mu\nu}$, the Minkowski metric. As said, this is dual to a CFT. To break conformal invariance while providing the mandatory harmonic oscillator form for $U(\zeta)$, a term $e^{\kappa^2 z_h^2}$ warping the AdS geometry is factored: $ds^2 = \frac{R^2}{z_h^2} e^{\kappa^2 z_h^2} (\eta_{\mu\nu} dx^\mu dx^\nu - dz_h^2)$. The action then becomes:

$$S_{HLF} = -\frac{1}{4} \int \sqrt{g} \frac{1}{\hat{a}^2} F^2 e^{\kappa^2 z_h^2} d^5 x. \quad (27)$$

As explained in Section 1.6, effective charges generalize the RGE running couplings by encapsulating, in addition to quantum loops, gluon radiation (higher-order DGLAP corrections), parton distribution correlations (higher-twists), and long-distance confinement effects. Accordingly, in Eq. (27), the $e^{\kappa^2 z_h^2}$ confinement term is attached to the coupling: $\alpha(z_h^2) \equiv \hat{a} e^{-\kappa^2 z_h^2/2}$ [113, 154–156]. Transforming $\alpha(z_h^2)$ to Minkowski 4-momentum space gives $\alpha_s^{\text{HLF}}(Q^2) = \alpha_s^{\text{HLF}}(0) e^{Q^2/4\kappa^2}$. The normalization $\alpha_s^{\text{HLF}}(0)$ is not provided by HLFQCD but determined by the scheme choice, e.g., the g_1 scheme [106] imposes:

$$\alpha_{g_1}^{\text{HLF}}(Q^2) = \pi e^{-Q^2/4\kappa^2}. \quad (28)$$

The normalization $\alpha_s^{\text{HLF}}(0)$ marks the effective charge dependence on an observable, similar to the RS-dependence of α_s^{pQCD} . The prediction, Eq. (28), has no free parameters and agrees well with data in the IR where HLFQCD is valid (Fig. 10).

One can interpolate between the IR Gaussian form, Eq. (28) and the UV log behavior, Eq. (21), with the form [52]:

$$\alpha_{g_1}^{\text{HLF}} = \pi \exp \left[- \int_0^{Q^2} \frac{du}{4k^2 + u \ln(u/\Lambda_s^2)} \right]. \quad (29)$$

Analytic continuation in the complex Q^2 -plane removes pQCD's Landau pole and, crucially, links κ to Λ_s . A simple Q^2 -dependence for κ determined by the meson spectrum, accounts for $m_q \neq 0$ [157]. The result is an analytic description of α_s at any Q^2 that agrees with IR and UV data, viz over more than 8 orders of magnitude: $2 \times 10^{-2} < Q^2 < 4.4 \times 10^{-6}$ GeV [157]. What happens to the Landau pole is revealing:

²³Most other effective charges have complicated interpretations, if any, and behaviors much different than expected from a force coupling: some, e.g., are negative.

²⁴Formally, the AdS \leftrightarrow CFT duality stems from the similitude between the group of isometries in 5D AdS and the SO(4,2) conformal group describing QCD if $m_q \rightarrow 0$.

²⁵Since the gravity theory is classical, HLFQCD is a semiclassical approximation to QCD. This makes HLFQCD strictly valid only in the IR, since in the UV, α_s runs due to quantum loops. Yet, we will see that HLFQCD can be smoothly merged with pQCD, providing a coupling valid at all Q^2 .

the pôle in Eq. (29) obeys $4\kappa^2 + Q^2 \ln(Q^2/\Lambda_s^2) = 0$. Continuation in the Q^2 -plane²⁶ shows that the Landau pôle (pQCD case, corresponding to $\kappa = 0$) on the real axis migrates to the imaginary Q^2 axis as κ increases. It reaches the imaginary axis (*maximum analyticity*) for

$$\kappa = \sqrt{2\pi}\Lambda_s/4. \quad (30)$$

The real-axis unphysical pôle has become an imaginary-axis physical feature exposing color confinement. From $\kappa = M_p/2$ and Eq. (30), $\Lambda_s^{g_1} = \sqrt{2/\pi}M_p$ in the g_1 scheme, which becomes²⁷ in $\overline{\text{MS}}$ $\Lambda_s^{\overline{\text{MS}}} = \sqrt{2/\pi}M_p e^{-\frac{2}{\beta_0}3.58} = 0.34 \text{ GeV}$ for $n_f = 3$, agreeing with the world data [1].

The Landau pôle metamorphosis from an unphysical feature to a manifestation of color confinement is naturally interpreted: imaginary pôles reveal dissipative/irreversible effects that suppress the time evolution of processes. For instance, the diverging oscillations of a driven harmonic oscillator are dissipated by friction formalized by an imaginary pôle in frequency space [158]. Oscillation dissipation suppresses the time evolution, *viz.*, the propagation, of the system. The larger the pôle's imaginary value, the larger the dissipation and, thus, the more the propagation is suppressed. Since α_s is a product of parton propagators; *e.g.*, Eq. (31), its pôle reflects pôles in parton propagators. Then, as the Landau pôle moves from real to complex to imaginary values, it suppresses parton propagation, eventually confining them (full propagation suppression) at the maximum analyticity condition.

1.8 Dyson-Schwinger equations

The DSE [159–161] are another approach providing α_s . The DSE are the equations of motion of QCD (or any QFT) and rigorously provide its correlation functions, *viz.* propagators and vertex functions. The DSE generate an infinite set of coupled non-linear integral equations, with the equation for the n -point function coupled to the equations for the $n+1$ or $n+2$ -point functions. In principle the DSE provide exact solutions but in practice, the infinite equation set must be limited (“truncated”). This must be done carefully, lest it creates unphysical artifacts. While this was historically a delicate issue, recent progress has identified symmetry-preserving schemes with controlled truncation-dependent uncertainties. To compute α_s with the DSE, one expresses it *via* renormalization “constants”, see Refs. [5, 6] for 1-loop UV computations of α_s . Consider $Z_\alpha(Q^2, \mu^2)$, the function that evolves α_s from an arbitrarily chosen renormalization scale μ to another scale Q^2 , *viz.* $Z_\alpha(Q^2, \mu^2) \equiv \alpha_s(\mu^2)/\alpha_s(Q^2)$. For, *e.g.*, the ghost-gluon vertex, $Z_\alpha = \tilde{Z}_1^2/(\tilde{Z}_3^2 Z_3)$, where, Z_3 , \tilde{Z}_1 , and \tilde{Z}_3 are the renormalization constants of the gluon propagator, ghost-gluon vertex, and ghost propagator, respectively. Computing α_s then amounts to computing the relevant Z s. Here, $Z_\alpha = \tilde{Z}_1^2/(\tilde{Z}_3^2 Z_3)$ provides α_s^{gh} , the ghost-gluon coupling²⁸ (Fig. 9):

$$\alpha_s^{\text{gh}}(Q^2) = \alpha_s^{\text{gh}}(\mu) G^2(Q^2, \mu) Z(Q^2, \mu), \quad (31)$$

where $G(Q^2, \mu)$ and $Z(Q^2, \mu)$ are respectively the ghost and gluon propagator dressing functions, which are calculable using the DSE.²⁹ Other vertices and associated renormalization constants can be used, yielding the 3-gluon coupling (α_s^{3g}), 4-gluon coupling (α_s^{4g}), and gluon-quark coupling (α_s^{gq}), see [6] for their formulae. Couplings can also be defined using single propagators, *e.g.*, the quark one [89]. These definitions yield couplings that typically differ in the IR. Even after selecting a vertex, couplings may still differ due to gauge and kinematic choices (*viz.*, what parton momentum-flow is considered [6]). We remind that in the UV, and for RS independent of m_q , the STI are valid, so all couplings identical. However, in the IR, they match only for formalisms enforcing the STI there, a constraint that has not been often pursued. Recent progress has now provided such a formalism. The resulting coupling is interpretable as a vertex/process-independent effective charge, and thus comparable to α_{g_1} , Eq. (24). This was achieved [3, 4] by making QCD's correlation functions to retrieve some of QED's abelian features.³⁰ Then, like for QED, vacuum polarization loops drive the running, consistent with the RGE. The resulting effective gluon dressing function $\mathcal{D}(Q^2)$ provides a universal, process-independent and effectively gauge-independent coupling $\hat{\alpha}_s$ [3, 4]:

$$\hat{\alpha}_s(Q^2)\mathcal{D}(Q^2) = \alpha_0 \left[\frac{G(Q^2; \mu^2)/G(0; \mu^2)}{1 - L(Q^2; \mu^2)G(Q^2; \mu^2)} \right]^2 \mathcal{D}(Q^2), \quad (32)$$

with $L(Q^2; \mu^2)$ the longitudinal component of the gluon-ghost vacuum polarization that vanishes at $Q^2 = 0$ and $\mathcal{D}(Q^2) \equiv \frac{Z(Q^2; \mu) m_g^2(Q^2; \mu)}{Q^2 m_0^2}$. The factor $m_g(Q^2, \mu)$ is interpreted as an effective running gluon mass that originates [162–164] from the Schwinger mechanism [165, 166]. Its magnitude is set by the IR limit $m_g \rightarrow m_0$, while in the UV, $m_g \rightarrow 0$ as it must. Then, $\mathcal{D}(Q^2)$ behaves as the propagator of a free, effectively massive, dressed gluon. The $m_g(Q^2, \mu)$ causes $\hat{\alpha}_s$ to lose its Q^2 -dependence in the IR, freezing at $\hat{\alpha}_0 = 0.97(4)\pi$, since for $Q \lesssim m_0$, the relevant scale becomes m_0 rather than Q . Following the concept of effective charge, Eq. (32) inserts in the coupling definition a renormalization group invariant interaction. In fact, the LHS of Eq. (32) expresses a force: $F = (\text{coupling} \times \text{propagator})$. Hence, it incorporates color confinement [8] like α_{g_1} , and can be compared to it. The ingredients of Eq. (32) were computed [4] by combining DSE results verified by LGT and, notwithstanding that $\hat{\alpha}_s(Q^2)$ has no adjustable parameters, it agrees well with α_{g_1} (Fig. 10).

1.9 Summary and Perspective

The QCD coupling α_s is a central ingredient of QCD and more generally, of the Standard Model. To understand it, vigorous efforts are ongoing on two separate fronts.

²⁶The continuation is permitted because α_{g_1} is an effective charge, thus an observable.

²⁷Eq. (3.39) of Ref. [6], with $v_2 = -3.58/\pi$ for $n_f = 3$, see Eq (25).

²⁸Also called *Taylor coupling* [80]. Being the easiest coupling that can be computed using correlation functions, it is prominent in the literature.

²⁹They are also conveniently calculated with LGT, the Functional Renormalization Group, pQCD (UV only), and other methods, see [6].

³⁰By systematically rearranging classes of diagrams so that their sums result in correlation functions that obey the STI.

The UV front is the pursuit of an accurate determination of $\alpha_s(M_Z)$. The techniques involved, the RGE and perturbation theory, are well-known. They yield an $\alpha_s(Q^2)$ that, at first order, logarithmically decreases with Q^2 . Thus, both α_s and its Q^2 -dependence vanish as $Q^2 \rightarrow \infty$, allowing to use pQCD to predict high-energy reactions, and proving that QCD is the correct gauge theory of the strong force. The current goal on the UV front is to determine $\alpha_s(M_Z)$ to well below the sub-percent accuracy [16]. Presently (2024), $\Delta\alpha_s/\alpha_s = 0.76\%$ [1]. This still makes $\Delta\alpha_s$ to contribute notably to uncertainties in pQCD calculations. Hence, hadronic uncertainties often dominate in calculations of Standard Model reactions, hindering not only studies of QCD and the Standard Model, but also searches for new physics. Reducing $\Delta\alpha_s$ necessitates combining many determinations of $\alpha_s(M_Z)$ both from distinct experiments and LGT. It also requires improving our knowledge of pQCD approximants to higher orders, and pursuing techniques that minimize pQCD ambiguities [167, 168]. To reach a satisfactory $\Delta\alpha_s$ will be a long quest, since even the sub-percent goal is far from our knowledge of the other fundamental couplings.³¹

The IR front is the study of α_s in the strongly-coupled QCD regime. Its challenges differ from those of the UV. **Firstly**, different definitions are available for α_s . **Secondly**, multiple couplings are often necessary to characterize QCD following how its different vertices couple. Such couplings tell us how quark, gluon and, if required, ghost fields interact at low energy in a given RS and gauge. Yet, they do not directly reflect QCD's strength, which is what is usually expected from a fundamental coupling. This particular hurdle is cleared by either making α_s an observable [83] or enforcing the Slavnov-Taylor identities [80, 81], QCD's equivalent of QED's Ward identities [43, 44]. While the former also ensures that α_s is finite and independent of RS and gauge, the latter usually does not. **Thirdly**, controlling the uncertainties of nonperturbative calculations or models is difficult. It has led to erroneous α_s behaviors arising from artifacts attached to under-controlled approximations. These challenges resulted in α_s predictions ranging from vanishing to diverging [20], hampering consensus on the IR behavior of α_s . To progress, a definition of α_s must be identified that provides a single, gauge-independent, RGE-compliant coupling whose meaning is clear, whose value reveals the quark-quark interaction strength at that Q^2 , and that is directly comparable to data. QED does this by defining α as an effective charge [24], which suggests to do the same for QCD [3, 83, 113]. Following this path produced not only consistent calculations for $\alpha_s(Q^2)$ once the RS-dependence is accounted for [20], but also agreement with the experimental data (Fig. 10). calculations and data reveal that α_s plateaus for $Q^2 \ll \Lambda_s^2$. Another character that the definition must display is practical usefulness: hadronic quantities must be calculable with the coupling. The aforementioned definition fulfills this as it enters the calculations of hadron masses, unpolarized, polarized and generalized parton distributions, form factors, meson decay constants, and characteristic scales such as Λ_s [51, 69, 169–183]. Overall, we now have a compelling candidate for an α_s that universally characterizes QCD's strength, that is gauge-, vertex-, and process-independent, and that can predict a wide range of nonperturbative hadronic quantities.

Acknowledgments

This work is supported by the U.S. Department of Energy, Office of Science, Office of Nuclear Physics, contract DE-AC05-06OR23177

References

- [1] R. L. Workman, et al., Review of Particle Physics, PTEP 2022 (2022) 083C01.
- [2] Luke W. Mo, Yung-Su Tsai, Radiative Corrections to Elastic and Inelastic e p and mu p Scattering, Rev. Mod. Phys. 41 (1969) 205–235, doi:10.1103/RevModPhys.41.205.
- [3] Daniele Binosi, Cedric Mezrag, Joannis Papavassiliou, Craig D. Roberts, Jose Rodríguez-Quintero, Process-independent strong running coupling, Phys. Rev. D 96 (2017) 054026.
- [4] Zhu-Fang Cui, Jin-Li Zhang, Daniele Binosi, Feliciano de Soto, Cédric Mezrag, Joannis Papavassiliou, Craig D. Roberts, Jose Rodríguez-Quintero, Jorge Segovia, Savvas Zafeiropoulos, Effective charge from lattice QCD, Chin. Phys. C 44 (8) (2020) 083102.
- [5] T. Muta, Foundations of quantum chromodynamics. Second edition. Lect. Notes. Phys. , vol. 57, World Scientific, Singapore 1998.
- [6] Alexandre Deur, Stanley J. Brodsky, Craig D. Roberts, QCD running couplings and effective charges, Prog. Part. Nucl. Phys. 134 (2024) 104081, doi:10.1016/j.pnpnp.2023.104081, 2303.00723.
- [7] Stanley J. Brodsky, Robert Shrock, Maximum Wavelength of Confined Quarks and Gluons and Properties of Quantum Chromodynamics, Phys. Lett. B 666 (2008) 95–99.
- [8] Daniele Binosi, Lei Chang, Joannis Papavassiliou, Craig D. Roberts, Bridging a gap between continuum-QCD and ab initio predictions of hadron observables, Phys. Lett. B 742 (2015) 183–188.
- [9] Daniele Binosi, Craig D. Roberts, Jose Rodríguez-Quintero, Scale-setting, flavor dependence, and chiral symmetry restoration, Phys. Rev. D 95 (11) (2017) 114009.
- [10] Daniele Binosi, Lei Chang, Joannis Papavassiliou, Si-Xue Qin, Craig D. Roberts, Natural constraints on the gluon-quark vertex, Phys. Rev. D 95 (3) (2017) 031501.
- [11] Fei Gao, Si-Xue Qin, Craig D. Roberts, Jose Rodriguez-Quintero, Locating the Gribov horizon, Phys. Rev. D 97 (3) (2018) 034010.
- [12] A. Deur, V. Burkert, J. P. Chen, W. Korsch, Experimental determination of the QCD effective charge $\alpha_{g_1}(Q)$, Particles 5 (2022) 171.
- [13] Stanley J. Brodsky, Alexandre Deur, Craig D. Roberts, The Secret to the Strongest Force in the Universe (2024).
- [14] S. Navas, et al. (Particle Data Group), Review of Particle Physics, Phys. Rev. D 110 (2024) 030001, doi:10.1103/PhysRevD.110.030001.
- [15] Franz Gross, et al., 50 Years of Quantum Chromodynamics, Eur. Phys. J. C 83 (2023) 1125, doi:10.1140/epjc/s10052-023-11949-2, 2212.11107.
- [16] D. d'Enterria, et al., The strong coupling constant: State of the art and the decade ahead (2022), 2203.08271.
- [17] Y. Aoki, et al., FLAG Review 2021, Eur. Phys. J. C 82 (10) (2022) 869.

³¹ $\Delta\alpha/\alpha = 1.5 \times 10^{-10}$, $\Delta\alpha_w/\alpha_w = 5.1 \times 10^{-7}$ and $\Delta G_N/G_N = 2.2 \times 10^{-5}$ [1].

- [18] David d'Enterria, et al., α_s (2019): Precision measurements of the QCD coupling α_s (2019): Precision measurements of the QCD coupling – arXiv:1907.01435 [hep-ph].
- [19] Antonio Pich, Juan Rojo, Rainer Sommer, Antonio Vairo, Determining the strong coupling: status and challenges, PoS Confinement2018 (2018) 035, doi:10.22323/1.336.0035.
- [20] Alexandre Deur, Stanley J. Brodsky, Guy F. de Teramond, The QCD Running Coupling, Prog. Part. Nucl. Phys. 90 (2016) 1–74.
- [21] G. Dissertori, The Determination of the Strong Coupling Constant, Adv. Ser. Direct. High Energy Phys. 26 (2016) 113–128, doi:10.1142/9789814733519.0006.
- [22] Guido Altarelli, The QCD Running Coupling and its Measurement, PoS Corfu2012 (2013) 002, doi:10.22323/1.177.0002.
- [23] G. M. Prospero, M. Raciti, C. Simolo, On the running coupling constant in QCD, Prog. Part. Nucl. Phys. 58 (2007) 387–438, doi:10.1016/j.pnpnp.2006.09.001.
- [24] Murray Gell-Mann, F. E. Low, Quantum electrodynamics at small distances, Phys. Rev. 95 (1954) 1300–1312.
- [25] Alexandre Deur, Stanley J. Brodsky, Guy F. de Teramond, On the Interface between Perturbative and Nonperturbative QCD, Phys. Lett. B 757 (2016) 275–281.
- [26] William Celmaster, Richard J. Gonsalves, QCD Perturbation Expansions in a Coupling Constant Renormalized by Momentum Space Subtraction, Phys. Rev. Lett. 42 (1979) 1435, doi:10.1103/PhysRevLett.42.1435.
- [27] William Celmaster, Richard J. Gonsalves, The Renormalization Prescription Dependence of the QCD Coupling Constant, Phys. Rev. D 20 (1979) 1420.
- [28] Gerard 't Hooft, Dimensional regularization and the renormalization group, Nucl. Phys. B 61 (1973) 455–468, doi:10.1016/0550-3213(73)90376-3.
- [29] H. Fritzsch, Murray Gell-Mann, H. Leutwyler, Advantages of the Color Octet Gluon Picture, Phys. Lett. B 47 (1973) 365–368, doi:10.1016/0370-2693(73)90625-4.
- [30] Sidney R. Coleman, David J. Gross, Price of asymptotic freedom, Phys. Rev. Lett. 31 (1973) 851–854.
- [31] Ernst Carl Gerlach Stueckelberg de Breidenbach, Andreas Petermann, Normalization of constants in the quanta theory, Helv. Phys. Acta 26 (1953) 499–520.
- [32] Curtis G. Callan, Jr., Broken scale invariance in scalar field theory, Phys. Rev. D 2 (1970) 1541–1547.
- [33] K. Symanzik, Small distance behavior in field theory and power counting, Commun. Math. Phys. 18 (1970) 227–246, doi:10.1007/BF01649434.
- [34] K. Symanzik, Small distance behavior analysis and Wilson expansion, Commun. Math. Phys. 23 (1971) 49–86, doi:10.1007/BF01877596.
- [35] David J. Gross, Frank Wilczek, Ultraviolet Behavior of Nonabelian Gauge Theories, Phys. Rev. Lett. 30 (1973) 1343–1346, doi:10.1103/PhysRevLett.30.1343.
- [36] H. David Politzer, Reliable Perturbative Results for Strong Interactions?, Phys. Rev. Lett. 30 (1973) 1346–1349, doi:10.1103/PhysRevLett.30.1346.
- [37] Howard D. Politzer, The Dilemma of Attribution, Nobel Lecture 2005, <https://www.nobelprize.org/prizes/physics/2004/politzer/lecture/>.
- [38] V. S. Vanyashin, M. V. Terentev, The Vacuum Polarization of a Charged Vector Field, Zh. Eksp. Teor. Fiz. 48 (2) (1965) 565–573.
- [39] I. B. Khriplovich, Green's functions in theories with non-abelian gauge group., Sov. J. Nucl. Phys. 10 (1969) 235–242.
- [40] Gerard 't Hooft, The Glorious days of physics: Renormalization of gauge theories (1998), hep-th/9812203.
- [41] Jean Zinn-Justin, Scholarpedia 5 (5) (2010) 8346.
- [42] L. D. Faddeev, V. N. Popov, Feynman Diagrams for the Yang-Mills Field, Phys. Lett. B 25 (1967) 29–30.
- [43] John Clive Ward, An Identity in Quantum Electrodynamics, Phys. Rev. 78 (1950) 182.
- [44] Y. Takahashi, On the generalized Ward identity, Nuovo Cim. 6 (1957) 371.
- [45] Einan Gardi, Georges Grunberg, Marek Karliner, Can the QCD running coupling have a causal analyticity structure?, JHEP 07 (1998) 007.
- [46] B. A. Kniehl, A. V. Kotikov, A. I. Onishchenko, O. L. Veretin, Strong-coupling constant with flavor thresholds at five loops in the anti-MS scheme, Phys. Rev. Lett. 97 (2006) 042001.
- [47] L. D. Landau, On analytic properties of vertex parts in quantum field theory, Nucl. Phys. 13 (1) (1959) 181–192, doi:10.1016/B978-0-08-010586-4.50103-6.
- [48] L. D. Landau, A. A. Abrikosov, I. M. Khalatnikov, An asymptotic expression for the photon Green function in quantum electrodynamics, Dokl. Akad. Nauk SSSR 95 (6) (1954) 1177–1180.
- [49] H. Leutwyler, On the history of the strong interaction, Mod. Phys. Lett. A 29 (2014) 1430023, doi:10.1142/S0217732314300237, 1211.6777.
- [50] William J. Marciano, Heinz Pagels, Quantum Chromodynamics: A Review, Phys. Rept. 36 (1978) 137, doi:10.1016/0370-1573(78)90208-9.
- [51] Alexandre Deur, Stanley J. Brodsky, Guy F. de Teramond, Connecting the Hadron Mass Scale to the Fundamental Mass Scale of Quantum Chromodynamics, Phys. Lett. B 750 (2015) 528–532.
- [52] Guy F. de Teramond, Arpon Paul, Stanley J. Brodsky, Alexandre Deur, Hans Günter Dosch, Tianbo Liu, Raza Sabbir Sufian (HLFHS), QCD Running Coupling in the Nonperturbative and Near-Perturbative Regimes, Phys. Rev. Lett. 133 (18) (2024) 181901, doi:10.1103/PhysRevLett.133.181901, 2403.16126.
- [53] Stanley J. Brodsky, Guy F. de Teramond, Hans Gunter Dosch, Joshua Erlich, Light-Front Holographic QCD and Emerging Confinement, Phys. Rept. 584 (2015) 1–105.
- [54] J.D. Bjorken, Emmanuel A. Paschos, Inelastic Electron Proton and gamma Proton Scattering, and the Structure of the Nucleon, Phys. Rev. 185 (1969) 1975–1982.
- [55] R. P. Feynman, The behavior of hadron collisions at extreme energies, Conf. Proc. C 690905 (1969) 237–258.
- [56] Yuri L. Dokshitzer, Calculation of the Structure Functions for Deep Inelastic Scattering and $e^+ e^-$ Annihilation by Perturbation Theory in Quantum Chromodynamics. (In Russian), Sov. Phys. JETP 46 (1977) 641–653.
- [57] V. N. Gribov, L. N. Lipatov, Deep inelastic electron scattering in perturbation theory, Phys. Lett. B 37 (1971) 78–80.
- [58] L. N. Lipatov, The parton model and perturbation theory, Sov. J. Nucl. Phys. 20 (1975) 94–102.
- [59] Guido Altarelli, G. Parisi, Asymptotic Freedom in Parton Language, Nucl. Phys. B 126 (1977) 298–318.
- [60] Antonio Pich, Precision physics with inclusive QCD processes, Prog. Part. Nucl. Phys. 117 (2021) 103846.
- [61] S. Bethke, et al. (2011), Workshop on Precision Measurements of α_s – arXiv:1110.0016 [hep-ph].
- [62] André H. Hoang, Christoph Regner, Borel representation of τ hadronic spectral function moments in contour-improved perturbation theory, Phys. Rev. D 105 (9) (2022) 096023.
- [63] D. Boito, F. Oliani, Renormalons in integrated spectral function moments and α_s extractions, Phys. Rev. D 101 (7) (2020) 074003.
- [64] Antonio Pich, Antonio Rodríguez-Sánchez, Determination of the QCD coupling from ALEPH τ decay data, Phys. Rev. D 94 (3) (2016) 034027.

- [65] Martin Luscher, Peter Weisz, Ulli Wolff, A Numerical method to compute the running coupling in asymptotically free theories, Nucl. Phys. B 359 (1991) 221–243.
- [66] Craig D. Roberts, Anthony G. Williams, Dyson-Schwinger equations and their application to hadronic physics, Prog. Part. Nucl. Phys. 33 (1994) 477–575.
- [67] S. Zafeiropoulos, P. Boucaud, F. De Soto, J. Rodríguez-Quintero, J. Segovia, Strong Running Coupling from the Gauge Sector of Domain Wall Lattice QCD with Physical Quark Masses, Phys. Rev. Lett. 122 (16) (2019) 162002.
- [68] Stanley J. Brodsky, Guy F. de Téramond, Hans Gunter Dosch, Cédric Lorcé, Universal Effective Hadron Dynamics from Superconformal Algebra, Phys. Lett. B 759 (2016) 171–177.
- [69] A. Deur, S. J. Brodsky, G. F. de Téramond, Determination of $\Lambda_{\overline{MS}}$ at five loops from holographic QCD, J. Phys. G 44 (10) (2017) 105005.
- [70] A. Accardi, et al., Electron Ion Collider: The Next QCD Frontier: Understanding the glue that binds us all, Eur. Phys. J. A 52 (9) (2016) 268.
- [71] T. Kutz, J. R. Pybus, D. W. Upton, C. Cotton, A. Deshpande, A. Deur, W. B. Li, D. Nguyen, M. Nycz, X. Zhen, High precision measurements of α_s at the future EIC (2024), 2406.05591.
- [72] Xurong Chen, Feng-Kun Guo, Craig D. Roberts, Rong Wang, Selected Science Opportunities for the EicC, Few Body Syst. 61 (4) (2020) 43.
- [73] Daniele P. Anderle, et al., Electron-ion collider in China, Front. Phys. (Beijing) 16 (6) (2021) 64701.
- [74] Richard Keith Ellis, et al. (2019), Physics Briefing Book: Input for the European Strategy for Particle Physics Update 2020–arXiv:1910.11775 [hep-ex].
- [75] A. Accardi, et al., Strong Interaction Physics at the Luminosity Frontier with 22 GeV Electrons at Jefferson Lab (2023), 2306.09360.
- [76] Craig D. Roberts, David G. Richards, Tanja Horn, Lei Chang, Insights into the emergence of mass from studies of pion and kaon structure, Prog. Part. Nucl. Phys. 120 (2021) 103883.
- [77] Yoichiro Nambu, G. Jona-Lasinio, Dynamical Model of Elementary Particles Based on an Analogy with Superconductivity. 1., Phys. Rev. 122 (1961) 345–358.
- [78] Kenneth D. Lane, Asymptotic Freedom and Goldstone Realization of Chiral Symmetry, Phys. Rev. D 10 (1974) 2605.
- [79] H. David Politzer, Effective Quark Masses in the Chiral Limit, Nucl. Phys. B 117 (1976) 397.
- [80] J. C. Taylor, Ward Identities and Charge Renormalization of the Yang-Mills Field, Nucl. Phys. B 33 (1971) 436–444.
- [81] A. A. Slavnov, Ward Identities in Gauge Theories, Theor. Math. Phys. 10 (1972) 99–107.
- [82] Murray Gell-Mann, F. E. Low, Quantum electrodynamics at small distances, Phys. Rev. 95 (1954) 1300–1312, doi:10.1103/PhysRev.95.1300.
- [83] G. Grunberg, Renormalization Scheme Independent QCD and QED: The Method of Effective Charges, Phys. Rev. D 29 (1984) 2315–2338, doi:10.1103/PhysRevD.29.2315.
- [84] Richard Williams, The quark-gluon vertex in Landau gauge bound-state studies, Eur. Phys. J. A 51 (5) (2015) 57, 1404.2545.
- [85] Anton K. Cyrol, Markus Q. Huber, Lorenz von Smekal, A Dyson–Schwinger study of the four-gluon vertex, Eur. Phys. J. C 75 (2015) 102, 1408.5409.
- [86] Veronique Bernard, Ulf-G. Meissner, Chiral perturbation theory, Ann. Rev. Nucl. Part. Sci. 57 (2007) 33–60, doi:10.1146/annurev.nucl.56.080805.140449, hep-ph/0611231.
- [87] Christoph Lerche, Lorenz von Smekal, On the infrared exponent for gluon and ghost propagation in Landau gauge QCD, Phys. Rev. D 65 (2002) 125006, doi:10.1103/PhysRevD.65.125006, hep-ph/0202194.
- [88] Philippe Boucaud, F. De Soto, A. Le Yaouanc, J. P. Leroy, J. Micheli, H. Moutarde, O. Pene, J. Rodriguez-Quintero, The Strong coupling constant at small momentum as an instanton detector, JHEP 04 (2003) 005.
- [89] John M. Cornwall, Dynamical Mass Generation in Continuum QCD, Phys. Rev. D 26 (1982) 1453, doi:10.1103/PhysRevD.26.1453.
- [90] William E. Caswell, Asymptotic Behavior of Nonabelian Gauge Theories to Two Loop Order, Phys. Rev. Lett. 33 (1974) 244.
- [91] A. I. Sanda, A Nonperturbative Determination of $\alpha(q^2)$ and Its Experimental Implications, Phys. Rev. Lett. 42 (1979) 1658, doi:10.1103/PhysRevLett.42.1658.
- [92] Tom Banks, A. Zaks, On the Phase Structure of Vector-Like Gauge Theories with Massless Fermions, Nucl. Phys. B 196 (1982) 189–204.
- [93] Yuri L. Dokshitzer, Valery A. Khoze, S. I. Troian, Specific features of heavy quark production. LPHD approach to heavy particle spectra, Phys. Rev. D 53 (1996) 89–119.
- [94] John L. Richardson, The Heavy Quark Potential and the Upsilon, J/ψ Systems, Phys. Lett. B 82 (1979) 272–274.
- [95] D. V. Shirkov, I. L. Solovtsov, Analytic model for the QCD running coupling with universal $\alpha_s(0)$ value, Phys. Rev. Lett. 79 (1997) 1209–1212.
- [96] E. Eichten, K. Gottfried, T. Kinoshita, John B. Kogut, K. D. Lane, Tung-Mow Yan, The Spectrum of Charmonium, Phys. Rev. Lett. 34 (1975) 369–372, [Erratum: Phys.Rev.Lett. 36, 1276 (1976)].
- [97] William Celmaster, Frank S. Henyey, The Quark - Anti-quark Interaction at All Momentum Transfers, Phys. Rev. D 18 (1978) 1688, doi:10.1103/PhysRevD.18.1688.
- [98] Robert Levine, Yukio Tomozawa, An Effective Potential for Heavy Quark - Anti-quark Bound Systems, Phys. Rev. D 19 (1979) 1572, doi:10.1103/PhysRevD.19.1572.
- [99] W. Buchmuller, G. Grunberg, S. H. H. Tye, The Regge Slope and the Lambda Parameter in QCD: An Empirical Approach via Quarkonia, Phys. Rev. Lett. 45 (1980) 103, doi:10.1103/PhysRevLett.45.103, [Erratum: Phys.Rev.Lett. 45, 587 (1980)].
- [100] J. D. Bjorken, S. H. H. Tye, Quarkonia and Quantum Chromodynamics, Phys. Rev. D 24 (1981) 132, doi:10.1103/PhysRevD.24.132.
- [101] S. Godfrey, Nathan Isgur, Mesons in a Relativized Quark Model with Chromodynamics, Phys. Rev. D 32 (1985) 189–231.
- [102] Yuri L. Dokshitzer, G. Marchesini, B. R. Webber, Dispersive approach to power behaved contributions in QCD hard processes, Nucl. Phys. B 469 (1996) 93–142, doi:10.1016/0550-3213(96)00155-1, hep-ph/9512336.
- [103] A. Deur, V. Burkert, Jian-Ping Chen, W. Korsch, Experimental determination of the effective strong coupling constant, Phys. Lett. B 650 (2007) 244–248.
- [104] A. Deur, V. Burkert, J. P. Chen, W. Korsch, Determination of the effective strong coupling constant $\alpha_s(g(1))(Q^2)$ from CLAS spin structure function data, Phys. Lett. B 665 (2008) 349–351, doi:10.1016/j.physletb.2008.06.049.
- [105] J. D. Bjorken, Asymptotic Sum Rules at Infinite Momentum, Phys. Rev. 179 (1969) 1547–1553, doi:10.1103/PhysRev.179.1547.
- [106] Stanley J. Brodsky, Hung Jung Lu, Commensurate scale relations in quantum chromodynamics, Phys. Rev. D 51 (1995) 3652–3668.
- [107] David J. Gross, Chris H. Llewellyn Smith, High-energy neutrino - nucleon scattering, current algebra and partons, Nucl. Phys. B 14 (1969) 337–347, doi:10.1016/0550-3213(69)90213-2.
- [108] S. B. Gerasimov, A Sum rule for magnetic moments and the damping of the nucleon magnetic moment in nuclei, Yad. Fiz. 2 (1965) 598–602.
- [109] S. D. Drell, Anthony C. Hearn, Exact Sum Rule for Nucleon Magnetic Moments, Phys. Rev. Lett. 16 (1966) 908–911.
- [110] G. Grunberg, Renormalization Group Improved Perturbative QCD, Phys. Lett. B 95 (1980) 70, [Erratum: Phys.Lett.B 110, 501 (1982)].

- [111] G. Grunberg, On Some Ambiguities in the Method of Effective Charges, *Phys. Rev. D* 40 (1989) 680.
- [112] L. F. Abbott, The Background Field Method Beyond One Loop, *Nucl. Phys. B* 185 (1981) 189–203.
- [113] Stanley J. Brodsky, Guy F. de Teramond, Alexandre Deur, Nonperturbative QCD Coupling and its β -function from Light-Front Holography, *Phys. Rev. D* 81 (2010) 096010.
- [114] J. D. Bjorken, Applications of the Chiral $U(6) \times (6)$ Algebra of Current Densities, *Phys. Rev.* 148 (1966) 1467–1478.
- [115] J. D. Bjorken, Inelastic Scattering of Polarized Leptons from Polarized Nucleons, *Phys. Rev. D* 1 (1970) 1376–1379.
- [116] V.N. Gribov, L.N. Lipatov, Deep inelastic e p scattering in perturbation theory, *Sov. J. Nucl. Phys.* 15 (1972) 438–450.
- [117] A. L. Kataev, The Ellis-Jaffe sum rule: The Estimates of the next to next-to-leading order QCD corrections, *Phys. Rev. D* 50 (1994) R5469–R5472.
- [118] A. L. Kataev, Deep inelastic sum rules at the boundaries between perturbative and nonperturbative QCD, *Mod. Phys. Lett. A* 20 (2005) 2007–2022, doi:10.1142/S0217732305018165.
- [119] P. A. Baikov, K. G. Chetyrkin, Johann H. Kuhn, Order α_s^4 (s) QCD Corrections to Z and tau Decays, *Phys. Rev. Lett.* 101 (2008) 012002.
- [120] A. Deur, Spin Sum Rules and the Strong Coupling Constant at large distance, *AIP Conf. Proc.* 1155 (1) (2009) 112–121.
- [121] A. Deur, Y. Prok, V. Burkert, D. Crabb, F. X. Girod, K. A. Griffioen, N. Guler, S. E. Kuhn, N. Kvaltine, High precision determination of the Q^2 evolution of the Bjorken Sum, *Phys. Rev. D* 90 (1) (2014) 012009.
- [122] A. Deur, et al., Experimental study of the behavior of the Bjorken sum at very low Q^2 , *Phys. Lett. B* 825 (2022) 136878.
- [123] K. Ackerstaff, et al., Measurement of the neutron spin structure function g_1^n with a polarized ^3He internal target, *Phys. Lett. B* 404 (1997) 383–389.
- [124] K. Ackerstaff, et al., Determination of the deep inelastic contribution to the generalized Gerasimov-Drell-Hearn integral for the proton and neutron, *Phys. Lett. B* 444 (1998) 531–538.
- [125] A. Airapetian, et al., Measurement of the proton spin structure function g_1^p with a pure hydrogen target, *Phys. Lett. B* 442 (1998) 484–492.
- [126] A. Airapetian, et al., Evidence for quark hadron duality in the proton spin asymmetry A_1 , *Phys. Rev. Lett.* 90 (2003) 092002.
- [127] A. Airapetian, et al., Precise determination of the spin structure function g_1 of the proton, deuteron and neutron, *Phys. Rev. D* 75 (2007) 012007.
- [128] J. H. Kim, et al., A Measurement of $\alpha_s(Q^2)$ from the Gross-Llewellyn Smith sum rule, *Phys. Rev. Lett.* 81 (1998) 3595–3598.
- [129] B. Adeva, et al., Measurement of the spin dependent structure function $g_1(x)$ of the deuteron, *Phys. Lett. B* 302 (1993) 533–539.
- [130] V. Yu. Alexakhin, et al., The Deuteron Spin-dependent Structure Function g_1^d and its First Moment, *Phys. Lett. B* 647 (2007) 8–17.
- [131] M. G. Alekseev, et al., The Spin-dependent Structure Function of the Proton g_1^p and a Test of the Bjorken Sum Rule, *Phys. Lett. B* 690 (2010) 466–472.
- [132] C. Adolph, et al., The spin structure function g_1^p of the proton and a test of the Bjorken sum rule, *Phys. Lett. B* 753 (2016) 18–28.
- [133] P. L. Anthony, et al., Determination of the neutron spin structure function., *Phys. Rev. Lett.* 71 (1993) 959–962.
- [134] K. Abe, et al., Precision measurement of the proton spin structure function g_1^p , *Phys. Rev. Lett.* 74 (1995) 346–350.
- [135] K. Abe, et al., Precision measurement of the deuteron spin structure function g_1^d , *Phys. Rev. Lett.* 75 (1995) 25–28.
- [136] K. Abe, et al., Measurements of the proton and deuteron spin structure function g_2 and asymmetry A_2 , *Phys. Rev. Lett.* 76 (1996) 587–591.
- [137] K. Abe, et al., Measurements of the Q^2 dependence of the proton and deuteron spin structure functions g_1^p and g_1^d , *Phys. Lett. B* 364 (1995) 61–68.
- [138] P. L. Anthony, et al., Deep inelastic scattering of polarized electrons by polarized ^3He and the study of the neutron spin structure, *Phys. Rev. D* 54 (1996) 6620–6650.
- [139] K. Abe, et al., Precision determination of the neutron spin structure function g_1^n , *Phys. Rev. Lett.* 79 (1997) 26–30.
- [140] K. Abe, et al., Measurement of the neutron spin structure function g_2^n and asymmetry A_2^n , *Phys. Lett. B* 404 (1997) 377–382.
- [141] K. Abe, et al., Next-to-leading order QCD analysis of polarized deep inelastic scattering data, *Phys. Lett. B* 405 (1997) 180–190.
- [142] K. Abe, et al., Measurements of the proton and deuteron spin structure functions g_1 and g_2 , *Phys. Rev. D* 58 (1998) 112003.
- [143] P. L. Anthony, et al., Measurement of the proton and deuteron spin structure functions g_2 and asymmetry A_2 , *Phys. Lett. B* 458 (1999) 529–535.
- [144] P. L. Anthony, et al., Measurement of the deuteron spin structure function $g_1^d(x)$ for $1 (\text{GeV}/c)^2 < Q^2 < 40 (\text{GeV}/c)^2$, *Phys. Lett. B* 463 (1999) 339–345.
- [145] P. L. Anthony, et al., Measurements of the Q^2 dependence of the proton and neutron spin structure functions g_1^p and g_1^n , *Phys. Lett. B* 493 (2000) 19–28.
- [146] P. L. Anthony, et al., Precision measurement of the proton and deuteron spin structure functions g_2 and asymmetries A_2 , *Phys. Lett. B* 553 (2003) 18–24.
- [147] Paul A. M. Dirac, Forms of Relativistic Dynamics, *Rev. Mod. Phys.* 21 (1949) 392–399.
- [148] Stanley J. Brodsky, Hans-Christian Pauli, Stephen S. Pinsky, Quantum chromodynamics and other field theories on the light cone, *Phys. Rept.* 301 (1998) 299–486.
- [149] Stanley J. Brodsky, Alexandre Deur, Craig D. Roberts, Artificial dynamical effects in quantum field theory, *Nature Rev. Phys.* 4 (7) (2022) 489–495.
- [150] Alexandre Deur, Stanley J. Brodsky, Craig D. Roberts, Bašić Terzić, Poincaré invariance, the Unruh effect, and black hole evaporation 2405.06002.
- [151] Guy F. de Teramond, Stanley J. Brodsky, Light-Front Holography: A First Approximation to QCD, *Phys. Rev. Lett.* 102 (2009) 081601, doi:10.1103/PhysRevLett.102.081601.
- [152] Juan Martin Maldacena, The Large N limit of superconformal field theories and supergravity, *Adv. Theor. Math. Phys.* 2 (1998) 231–252.
- [153] Amanda W. Peet, Joseph Polchinski, UV / IR relations in AdS dynamics, *Phys. Rev. D* 59 (1999) 065011, doi:10.1103/PhysRevD.59.065011, hep-th/9809022.
- [154] H. J. Pirner, B. Galow, Strong Equivalence of the AdS-Metric and the QCD Running Coupling, *Phys. Lett. B* 679 (2009) 51–55, doi: 10.1016/j.physletb.2009.07.009, 0903.2701.
- [155] U. Gursoy, E. Kiritsis, Exploring improved holographic theories for QCD: Part I, *JHEP* 02 (2008) 032, doi:10.1088/1126-6708/2008/02/032, 0707.1324.
- [156] U. Gursoy, E. Kiritsis, F. Nitti, Exploring improved holographic theories for QCD: Part II, *JHEP* 02 (2008) 019, doi:10.1088/1126-6708/2008/02/019, 0707.1349.
- [157] Hans Günter Dosch, Guy F. de Teramond, Arpon Paul, Stanley J. Brodsky, Alexandre Deur, Tianbo Liu, Raza Sabbir Sufian (HLFHS), In preparation 2025.
- [158] George B Arfken, Hans J Weber, *Mathematical methods for physicists*; 7th ed., Academic Press, San Diego, CA 2012, URL <https://www.sciencedirect.com/book/9780123846549/mathematical-methods-for-physicists>.

- [159] F. J. Dyson, The S matrix in quantum electrodynamics, *Phys. Rev.* 75 (1949) 1736–1755.
- [160] Julian S. Schwinger, On the Green's functions of quantized fields. 1, *Proc. Nat. Acad. Sci.* 37 (1951) 452–455.
- [161] Julian S. Schwinger, On the Green's functions of quantized fields. 2, *Proc. Nat. Acad. Sci.* 37 (1951) 455–459.
- [162] Daniele Binosi, Emergent Hadron Mass in Strong Dynamics, *Few Body Syst.* 63 (2) (2022) 42.
- [163] J. Papavassiliou, Emergence of mass in the gauge sector of QCD, *Chin. Phys. C* 46 (11) (2022) 112001.
- [164] A. C. Aguilar, F. De Soto, M. N. Ferreira, J. Papavassiliou, F. Pinto-Gómez, C. D. Roberts, J. Rodríguez-Quintero, Schwinger mechanism for gluons from lattice QCD, *Phys. Lett. B* 841 (2023) 137906, doi:10.1016/j.physletb.2023.137906.
- [165] Julian S. Schwinger, Gauge Invariance and Mass, *Phys. Rev.* 125 (1962) 397–398.
- [166] Julian S. Schwinger, Gauge Invariance and Mass. 2., *Phys. Rev.* 128 (1962) 2425–2429.
- [167] Stanley J. Brodsky, G. Peter Lepage, Paul B. Mackenzie, On the Elimination of Scale Ambiguities in Perturbative Quantum Chromodynamics, *Phys. Rev. D* 28 (1983) 228.
- [168] Stanley J. Brodsky, Xing-Gang Wu, Scale Setting Using the Extended Renormalization Group and the Principle of Maximum Conformality: the QCD Coupling Constant at Four Loops, *Phys. Rev. D* 85 (2012) 034038, [Erratum: *Phys. Rev. D* 86, 079903 (2012)].
- [169] Lei Chang, Craig D. Roberts, Tracing masses of ground-state light-quark mesons, *Phys. Rev. C* 85 (2012) 052201.
- [170] Guy F. de Téramond, Tianbo Liu, Raza Sabbir Sufian, Hans Günter Dosch, Stanley J. Brodsky, Alexandre Deur, Universality of Generalized Parton Distributions in Light-Front Holographic QCD, *Phys. Rev. Lett.* 120 (18) (2018) 182001.
- [171] Guy F. de Téramond, H. G. Dosch, Tianbo Liu, Raza Sabbir Sufian, Stanley J. Brodsky, Alexandre Deur, Gluon matter distribution in the proton and pion from extended holographic light-front QCD, *Phys. Rev. D* 104 (11) (2021) 114005, doi:10.1103/PhysRevD.104.114005.
- [172] Lei Chang, I. C. Cloet, J. J. Cobos-Martinez, C. D. Roberts, S. M. Schmidt, P. C. Tandy, Imaging dynamical chiral symmetry breaking: pion wave function on the light front, *Phys. Rev. Lett.* 110 (13) (2013) 132001.
- [173] Chao Shi, Chen Chen, Lei Chang, Craig D. Roberts, Sebastian M. Schmidt, Hong-Shi Zong, Kaon and pion parton distribution amplitudes to twist-three, *Phys. Rev. D* 92 (2015) 014035, doi:10.1103/PhysRevD.92.014035.
- [174] Minghui Ding, Fei Gao, Lei Chang, Yu-Xin Liu, Craig D. Roberts, Leading-twist parton distribution amplitudes of S-wave heavy-quarkonia, *Phys. Lett. B* 753 (2016) 330–335, doi:10.1016/j.physletb.2015.11.075.
- [175] Minghui Ding, Khépani Raya, Daniele Binosi, Lei Chang, Craig D. Roberts, Sebastian M. Schmidt, Drawing insights from pion parton distributions, *Chin. Phys. C* 44 (3) (2020) 031002, doi:10.1088/1674-1137/44/3/031002.
- [176] Minghui Ding, Khépani Raya, Daniele Binosi, Lei Chang, Craig D. Roberts, Sebastian M. Schmidt, Symmetry, symmetry breaking, and pion parton distributions, *Phys. Rev. D* 101 (5) (2020) 054014, doi:10.1103/PhysRevD.101.054014.
- [177] Pei-Lin Yin, Yin-Zhen. Xu, Zhu-Fang Cui, Craig D. Roberts, José Rodríguez-Quintero, All-Orders Evolution of Parton Distributions: Principle, Practice, and Predictions, *Chin. Phys. Lett.* 40 (9) (2023) 091201, doi:10.1088/0256-307X/40/9/091201.
- [178] Raza Sabbir Sufian, Guy F. de Téramond, Stanley J. Brodsky, Alexandre Deur, Hans Günter Dosch, Analysis of nucleon electromagnetic form factors from light-front holographic QCD : The spacelike region, *Phys. Rev. D* 95 (1) (2017) 014011.
- [179] K. Raya, L. Chang, A. Bashir, J. J. Cobos-Martinez, L. X. Gutiérrez-Guerrero, C. D. Roberts, P. C. Tandy, Structure of the neutral pion and its electromagnetic transition form factor, *Phys. Rev. D* 93 (7) (2016) 074017.
- [180] Khepani Raya, Minghui Ding, Adnan Bashir, Lei Chang, Craig D. Roberts, Partonic structure of neutral pseudoscalars via two photon transition form factors, *Phys. Rev. D* 95 (7) (2017) 074014, doi:10.1103/PhysRevD.95.074014.
- [181] Jose Rodríguez-Quintero, Daniele Binosi, Cédric Mezrag, Joannis Papavassiliou, Craig D. Roberts, Process-independent effective coupling. From QCD Green's functions to phenomenology, *Few Body Syst.* 59 (6) (2018) 121.
- [182] Zhen-Ni Xu, Zhao-Qian Yao, Si-Xue Qin, Zhu-Fang Cui, Craig D. Roberts, Bethe–Salpeter kernel and properties of strange-quark mesons, *Eur. Phys. J. A* 59 (3) (2023) 39.
- [183] Hans Günter Dosch, Guy F. de Téramond, Tianbo Liu, Raza Sabbir Sufian, Stanley J. Brodsky, Alexandre Deur, Towards a single scale-dependent Pomeron in holographic light-front QCD, *Phys. Rev. D* 105 (3) (2022) 034029.